

# Cyclic Adsorption Processes

## Gas Phase Separation Processes

### Pressure Swing Adsorption: Biogas Upgrading

**KEYWORDS:** Biogas / Pressure Swing Adsorption / Gas Separation

To perform the separation of CO<sub>2</sub>, the process known as biogas upgrading, several technologies have been studied. Adsorption-based processes or membrane separation are some of the alternatives to liquid amine absorption, the one utilized nowadays in the industry. In this topic, the activities focused on evaluating new materials and/or new processes to enhance the performance of adsorption-based processes for biogas upgrade. Adsorption equilibrium isotherms and adsorption kinetics were assessed experimentally, while new processes were designed through numerical simulations.

#### Introduction and Objectives

Biogas is obtained by anaerobic digestion of diverse materials such as manure, crops, and food industry wastes. Depending on the source, its composition may vary, but it contains mainly carbon dioxide (more than 30%) and methane (about 60%). Then, biogas needs to be transformed into biomethane (CO<sub>2</sub> separation) for applications that imply the transport of liquefied CH<sub>4</sub> (LBG), since methane needs to be compressed. In order to perform the separation of CO<sub>2</sub>, the process known as biogas upgrading, several technologies have been studied, such as adsorption-based technologies. Suitable materials to be employed in these processes for the selective adsorption of carbon dioxide from biogas streams have been studied.

#### Current Development

The focus of current research and development efforts lies in optimizing and expanding the use of adsorption processes, leveraging materials such as carbons, zeolites, and metal-organic frameworks.

A carbon xerogel obtained by carbonization of a resorcinol-formaldehyde polymer which was synthesized using Cs<sub>2</sub>CO<sub>3</sub> as catalyst was employed as CO<sub>2</sub> selective adsorbent for biogas upgrading (see Figure 1). Equilibrium studies showed a large CO<sub>2</sub> uptake ( $q_{\text{sat}}=6.57 \text{ mol kg}^{-1}$  and  $\Delta H_{\text{ads}}=-28.4 \text{ kJ mol}^{-1}$ ) compared to the CH<sub>4</sub> one ( $q_{\text{sat}}=3.83 \text{ mol kg}^{-1}$  and  $\Delta H_{\text{ads}}=-19.6 \text{ kJ mol}^{-1}$ ) revealing a high CO<sub>2</sub> to CH<sub>4</sub> selectivity, especially at low pressures.

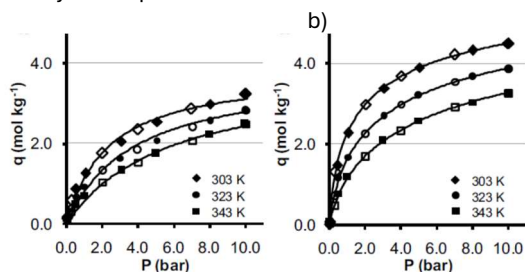


Fig 1. Adsorption (close) and desorption (open) isotherms of a) CH<sub>4</sub> and b) CO<sub>2</sub>. The lines represent the Langmuir/Toth fitting.

The adsorption equilibrium and kinetics of CO<sub>2</sub>, CH<sub>4</sub>, and N<sub>2</sub> on three types of BETA zeolites, Na-BETA-25, H-BETA,25, and H-BETA-150, were investigated at different temperatures and a defined partial pressure range from dynamic breakthrough experiments. The adsorbed amount followed the decreasing order of CO<sub>2</sub> > CH<sub>4</sub> > N<sub>2</sub> for all studied materials. For the same ratio of SiO<sub>2</sub>/Al<sub>2</sub>O<sub>3</sub>, the Na-BETA-25 zeolite showed a higher uptake capacity than H-BETA-25, due to the presence of a Na<sup>+</sup> cationic center. Comparing the same H<sup>+</sup> compensation cation,

zeolite H-BETA-25 expressed a slightly higher adsorption capacity than H-BETA-150. Regarding the selectivity of gases, based on their affinity constants, H-BETA-150 displayed the best performance.

The adsorption of CO<sub>2</sub>, CH<sub>4</sub> and N<sub>2</sub> in binderless zeolite 4A spheres with different sizes (4A BFK 2.5–5.0 mm, 4A BFK 1.6–2.5 mm) as well as different (higher) bulk density (4A BFK 1.6–2.5 mm HSD) was studied. The adsorption equilibrium isotherms were measured using a gravimetric method at 303, 343, and 373 K, demonstrating that the adsorption equilibrium of all zeolites 4A samples was equally well described by the same model when the adsorption capacity is given in terms of the mass of adsorbent which was expected since the three samples have the same type of crystals. When the adsorption capacity is described by the volume of adsorbent, the high bulk density sample presents a significantly higher value. The advantages of the denser material in terms of adsorption capacity are evident, significantly smaller process unit can be used.

Figure 2 shows the three 4A samples studied and the performed characterization.

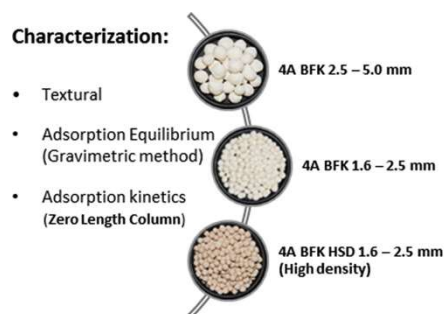


Fig 2. Three 4A samples measured: BFK 2.5 – 5.0 mm, BFK 1.6 – 2.5 mm and BFK HSD 1.6 – 2.5 mm (high density).

Figure 3 presents the results of CO<sub>2</sub> adsorption equilibrium isotherms measurements at 303 K for the three samples, and the results of CH<sub>4</sub> adsorption equilibrium isotherms measurements at 303, 343 and 373 K on zeolite 4A BFK 1.6 – 2.5 mm.

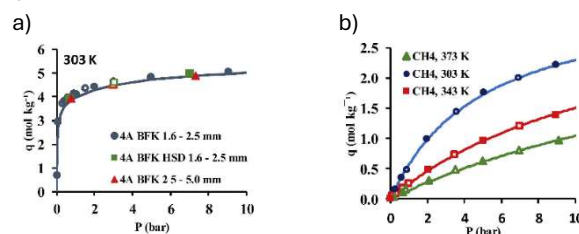


Fig 3. a) CO<sub>2</sub> adsorption equilibrium isotherms on 4A BFK 1.6–2.5 mm, 4A BFK 2.5–5.0 mm and 4A BFK HSD 1.6–2.5 mm; b) Adsorption equilibrium isotherms of CH<sub>4</sub> on 4A BFK 1.6–2.5 mm zeolite.

Single- and multicomponent adsorption fixed bed breakthrough experiments of carbon dioxide (CO<sub>2</sub>), methane (CH<sub>4</sub>), and nitrogen (N<sub>2</sub>) on commercial binder-free beads of 4A zeolite have been studied. The ternary experiments (CO<sub>2</sub>/CH<sub>4</sub>/N<sub>2</sub>) show a practically complete separation of CO<sub>2</sub> from CH<sub>4</sub>/N<sub>2</sub> at all the temperatures studied, with selectivity at 313 K around 24 of CO<sub>2</sub> over CH<sub>4</sub>, and 50 over N<sub>2</sub>. The results

showed in the present work evidence that the binder-free beads of zeolite 4A can be employed to efficiently separate CO<sub>2</sub> from CO<sub>2</sub>/CH<sub>4</sub>/N<sub>2</sub> mixtures by fixed bed adsorption.

The adsorption of CO<sub>2</sub>, CH<sub>4</sub>, and N<sub>2</sub> has been studied on potassium-exchanged (95%) binder-free beads of Y zeolite through single, binary, and ternary fixed bed breakthrough experiments, covering the temperature range between 313 and 423 K and a pressure of up to 350 kPa. At 313 K and 350 kPa, the single-component data obtained showed that the amounts adsorbed of CO<sub>2</sub>, CH<sub>4</sub>, and N<sub>2</sub> are around 6.42, 1.45, and 0.671 mol kg<sup>-1</sup>, respectively. The binary experiments CO<sub>2</sub>/N<sub>2</sub> carried out under typical post-combustion conditions show a selectivity of CO<sub>2</sub> over N<sub>2</sub> around 104. The ternary experiments resulted in the selectivities of CO<sub>2</sub> over CH<sub>4</sub> and N<sub>2</sub> around 19 and 45, respectively. The results show that the potassium-exchanged binder-free beads of Y zeolite enhance the amount adsorbed of CO<sub>2</sub> at low partial pressure over other alkali metal-exchanged faujasites and efficiently separate it from binary (CO<sub>2</sub>/N<sub>2</sub>) and ternary (CO<sub>2</sub>/CH<sub>4</sub>/N<sub>2</sub>) mixtures by fixed bed adsorption.

A multistep PSA process to obtain high-purity CO<sub>2</sub>, CH<sub>4</sub>, and syngas products resulting from the CO<sub>2</sub> electroreduction reaction was studied. NaX and MFI zeolites were selected because of their affinity for CO<sub>2</sub> and CH<sub>4</sub>, respectively, based on Monte Carlo and molecular dynamic simulations, considering pore sizes, topologies, and chemical compositions of a set of adsorbents. Two alternative configurations for the dual PSA were studied, with the order in which the separation of CO<sub>2</sub>/CH<sub>4</sub>/syngas occurring being their main difference. In case study 1, the CO<sub>2</sub> contained in the feed mixture is retained in the NaX zeolite in the first PSA, and then methane is separated from the syngas stream in a second PSA using the MFI zeolite. The simulation results showed that the proposed dual-PSA process for case study 1 is capable of obtaining CO<sub>2</sub> with high purity and recovery (99.1 and 95.1%, respectively) but produces methane with a purity below the required one for it to be used as domestic gas (90.5 vs 97%) despite the high methane recovery that is achieved (95.2%). It can also be concluded that the produced methane can be instead injected into the natural gas grid in some European countries (e.g., France and Netherlands). As for case study 2, a mixture mostly composed of CO<sub>2</sub> and methane is separated from the syngas stream in a first PSA with the use of the MFI zeolite, and afterward, CO<sub>2</sub> is removed from methane using NaX zeolite in a second PSA. It is possible to conclude that the methane and CO<sub>2</sub> products can be obtained in the proposed dual-PSA process for case study 2 with purity above 97% and a high recovery (i.e., >95% for CH<sub>4</sub> and >98% for CO<sub>2</sub>). This case study meets the required methane specifications for it to be used as domestic gas. However, a much higher value for the energy consumption of this process (64.9 W.h.mol<sub>CH<sub>4</sub></sub><sup>-1</sup>) is observed when compared to the proposed process of case study 1 (29.8 W.h.mol<sub>CH<sub>4</sub></sub><sup>-1</sup>).

Figure 4 presents the scheme of the two stages of the PSA process.

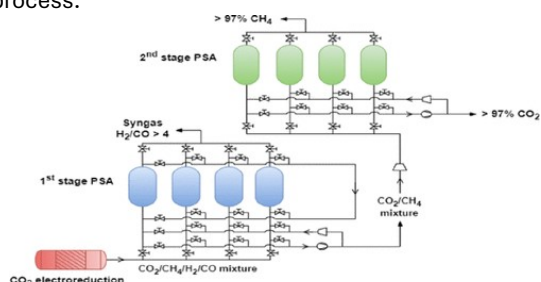


Fig 4. Two stages of PSA processes to obtain high-purity methane, CO<sub>2</sub>, and syngas.

The microporous bioderived Al dicarboxylate MIL-160(Al) MOF in its shaped form has been evaluated as a candidate for biogas upgrading (BU) and/or carbon capture and storage (CCS) by studying adsorption isotherms of CO<sub>2</sub>, CH<sub>4</sub>, and N<sub>2</sub> at 313, 343, and 373 K until 8 bar. The isotherms disclosed the following loading capacities: 4.2 (CO<sub>2</sub>), 2.07 (CH<sub>4</sub>), and 0.69 (N<sub>2</sub>) mol kg<sup>-1</sup> at 5.8 bar and 313 K. Breakthrough curve experiments with mixtures CO<sub>2</sub>/CH<sub>4</sub> and CO<sub>2</sub>/N<sub>2</sub> at the optimum selectivity conditions were developed and simulated using ASPEN Adsorption. This work demonstrates the potential of MIL-160(Al) to be used in BU- and/or CCS-related applications.

### Future Perspectives

The emphasis on developing efficient and low-cost adsorption processes underscores the importance of obtaining fundamental data such as adsorption equilibrium isotherms, kinetics, selectivities, and cost for large-scale design and implementation.

The importance of biogas as a renewable energy source, the challenges posed by GHG emissions, and the ongoing efforts to develop effective and economical technologies for biogas upgrading, contribute to the broader goal of mitigating climate change.

### Related Sustainable Development Goals



#### Outputs

##### Master Dissertations

- [1] Daniela G. B. Morence, A study on methane and carbon dioxide adsorption, MIEQ, FEUP, 2019
- [2] Carina S. R. Sá, Developing a technological concept for the removal of Siloxanes and VOCs from landfill gas, MIEQ, FEUP, 2021
- [3] Anita M. Barbosa, Captura e armazenamento de CO<sub>2</sub> resultante da exaustão de unidades de purificação de biogás, MIEQ, FEUP, 2022
- [4] Daniela A. Gonçalves, Liquefaction of CO<sub>2</sub> from a Biogas Upgrading Plant for Food-Grade Applications, MIEQ, FEUP, 2022
- [5] Ana M. R. F. Baptista, Thermal Swing Adsorption Technology Development for VOCs and Siloxanes Removal, MIEQ, FEUP, 2022
- [6] Fellipe A. Silva, Developing a technological concept for the removal of VOCs and Siloxanes from a landfill gas: Solvent Recovery, MIEQ, FEUP, 2022
- [7] Miguel F. R. P. G. Cabral, Techno-economic study of multi-stage membrane configurations for biogas upgrading with 0.2% methane slip, MIEQ, FEUP, 2022
- [8] Bruno C. Rodrigues, Methane and CO<sub>2</sub> recovery from the purge stream to design a closed-loop for the Biogas upgrading plant, MIEQ, FEUP, 2022

##### Selected Publications

- [1] J. F. Vivo-Vilches *et al.*, Ind. Eng. Chem. Res. 62, 169–177 (2018)
- [2] A. Henrique *et al.*, Chem Eng Technology 42, 327–342 (2018)
- [3] R. Seabra *et al.*, Micro Meso Materials. 277, 105–114 (2019)
- [4] L. F. A. S. Zafanelli *et al.*, Ind. Eng. Chem. Res. 59, 13724–13734 (2020)
- [5] M. Karimi *et al.*, Chem Eng. Journal 425, 130538 (2020)
- [6] Aly E. *et al.*, Ind. Eng. Chem. Res. 60, 15236–15247 (2021)
- [7] M. C.N. Bessa *et al.*, Ind. Eng. Chem. Res. 62, 8847–8863 (2023)
- [8] M. Karimi *et al.*, Ind. Eng. Chem. Res. 62, 5216–5229 (2023)

##### Team

Alírio E. Rodrigues, Emeritus Professor; Alexandre Ferreira, Assitant Professor / Group Leader; Ana Mafalda Ribeiro, Assistant Professor; Maria João Regufe, PostDoc Researcher; Paulo Carmo, PostDoc Researcher; Mohsen Karimi, Ph.D. Student; Lucas Zafanelli, Ph.D. Student; Mariana Bessa, Ph.D. Student; Adriano Henrique, Ph.D. Student; Jose F. Vivo-Vilches, Visiting Ph.D. Student; Rute Seabra, M.Sc. Student.

##### Funding

LSRE-LCM Base Funding, UIDB/50020/2020, 2020-2023  
 LSRE-LCM Programmatic Funding, UIDP/50020/2020, 2020-2023  
 LA LSRE-LCM Funding, UID/EQU/50020/2019, 2019  
 LA LSRE-LCM Funding, POI-01-0145-FEDER-006984, 2013-2018  
 Project POCI-01-0145-FEDER-006984, 2018-2023  
 Project AIProcMat@N2020, NORTE-01-0145-FEDER-000006, 2016-2019  
 Project VALORCOMP, 0119\_VALOR-COMP\_2\_P, 2014-2020  
 PTDC 2020 3599-PPCDTI  
 PTDC/EQU-EPQ/0467/2020  
 Project HyGreen&LowEmissions NORTE-01-0145-FEDER-000077  
 SFRH/BD/140550/2018, SFRH/BD/148525/2019, DFA/BD/7925/2020, 2022.10166.BD

# Cyclic Adsorption Processes

## Gas Phase Separation Processes

### Pressure Swing Adsorption: CO<sub>2</sub> capture

**KEYWORDS:** Carbon dioxide capture / Pressure Swing Adsorption / Gas Separation

This topic outlines various studies on different materials for carbon capture using Pressure Swing Adsorption. The reported studies explore a range of materials for CO<sub>2</sub> capture, assessing their effectiveness and feasibility.

#### Introduction and Objectives

Increasing greenhouse gas emissions contributing to global climate change is a major concern of environmental protection. One of the main responsible is carbon dioxide. Adsorption technology not only is an eco-friendly technology but also represents a low-energy consumption process, which can selectively separate carbon dioxide in an efficient way. Accordingly, recently it has received significant attention regarding its applications for carbon capture and storage, as well as biogas upgrading. Lately, many efforts have been conducted to optimize the carbon dioxide adsorption process, reducing energy consumption, consequently decreasing the operating cost, as well as developing sustainable sorbents for carbon capture.

#### Current Development

The microstructure effect of carbon materials on the low-concentration methane adsorption separation from its mixture with nitrogen was investigated. The granular coconut shell-activated carbons (GACs) with high CH<sub>4</sub> adsorption capacity and good CH<sub>4</sub>/N<sub>2</sub> selectivity were prepared. Adsorption equilibrium isotherms of CH<sub>4</sub> and N<sub>2</sub> and breakthrough experiments for pure (N<sub>2</sub>/He and CH<sub>4</sub>/He) and binary (CH<sub>4</sub>/N<sub>2</sub>/He) components were performed. A four-step one-bed vacuum pressure swing adsorption (VPSA) process was adopted, demonstrating that the low-concentration methane can be enriched, but methane purity in product gas is still limited by the CH<sub>4</sub>/N<sub>2</sub> selectivity on GAC.

Derived composts from Municipal Solid Wastes (MSWs) are considered a source of adsorbents for CO<sub>2</sub> capture by synthesizing five different samples. Then, screening studies were performed in an adsorption breakthrough apparatus to find the best synthesized sample regarding CO<sub>2</sub> uptake (see Figure 1). Thereafter, a mathematical model is developed to match the breakthrough curves of the best screened samples being also applied to simulate a pressure swing adsorption cycle to evaluate the capability and feasibility of the best AC sample synthesized for cyclic CO<sub>2</sub> purification using adsorption processes. It was verified that MSWC can be successfully employed to remove CO<sub>2</sub> from flue gas using PSA cyclic adsorption processes.

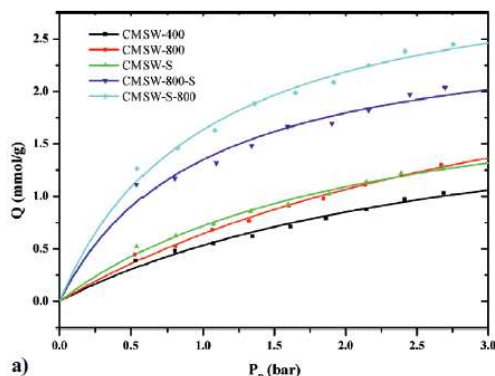


Fig 1. Experimental equilibrium data (symbols) and fitted Langmuir isotherm (lines) for CO<sub>2</sub> adsorption at 40 C; of investigated adsorbents.

Also, low-cost geopolymers were developed by partially replacing metakaolin with residues (fly ash, rice husk ash, and calcined rice husk ash – Figure 2) for use in the CO<sub>2</sub> capture process. The work demonstrated that the most promising geopolymeric material produced using fly ash, metakaolin, and NaOH (as an alkaline activator) (MF-1) resulted in suitable CO<sub>2</sub> adsorption capacity, high compressive strength, and regeneration performance.

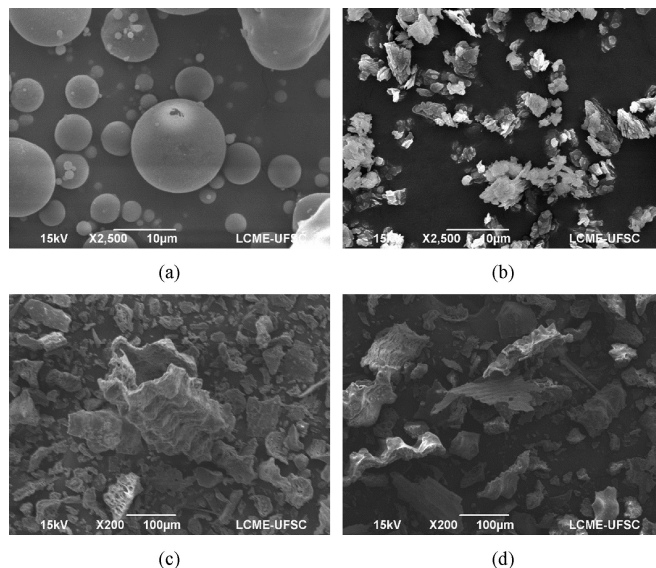


Fig 2. Morphology of different materials used in this study: (a) fly ash; (b) metakaolin; (c) rice husk ash; (d) calcined rice husk ash.

The effect of amine (MEA, DEA, and TEA) functionalization of high surface area supports (Amberlite IR120H, Ambersep 252H, Amberlite 200CNa, and Amberlite XAD7HP) on adsorption of CO<sub>2</sub> from gases streams were evaluated.

The experiments of ethanolamines impregnation revealed that the mass of amine incorporated into the different resins was generally not dependent on the studied amination variables, on the mass loss in the pretreatment with methanol, on the moisture holding capacity of the resins, on the efficiency of water removal in the pretreatment with methanol, and the type of resin in terms of structure (gel or macroreticular) and capability to exchange ions.

The potential of two 3D-printed activated carbons with different activation times (M1<M2) has been investigated for their use in CO<sub>2</sub> capture in post-combustion streams. A series of fixed-bed breakthrough adsorption experiments were performed in a wide range of temperature and pressure of interest for post-combustion applications, namely: between 313 and 373 K and the partial pressure up to 120 kPa. The adsorption equilibrium and heat of adsorption in both monoliths follow the order CO<sub>2</sub> >> N<sub>2</sub>. Both materials presented excellent stability and regenerability over consecutive adsorption-desorption experiments. The mathematical model used in this work describes well the adsorption and desorption breakthrough curves data. Finally, the present work indicates that the 3D-printed activated carbon (Figure 3) can be used in a temperature swing adsorption process for CO<sub>2</sub> capture.

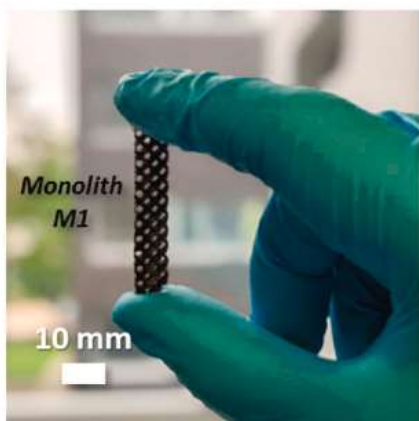


Fig 3. Activated carbon 3D-printed (M1).

Also, a study focuses on the modeling of a sorptive unit for CO<sub>2</sub> capture at high temperatures, considering as a case-study the data obtained from experiments using a conventional post-combustion stream from coal power plants (15% CO<sub>2</sub>/85% N<sub>2</sub> at 623 K and 134 kPa) was performed. A one-dimensional (1D) heterogeneous dynamic fixed-bed model able to predict the CO<sub>2</sub> equilibrium and kinetics of adsorption on a K-promoted hydrotalcite was successfully developed and implemented in gPROMS<sup>®</sup> software. As illustrated in Figure 4 (cycles 0 to 5), the experimental breakthrough curves of CO<sub>2</sub> are predicted quite well by the model.

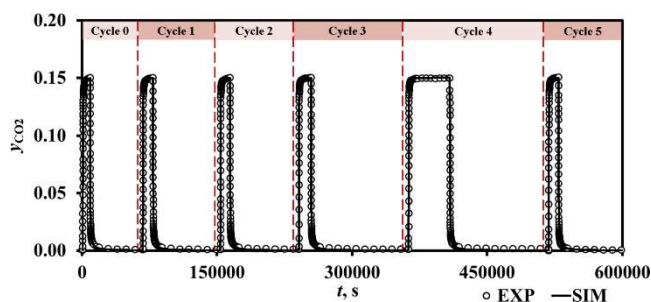


Fig 4. The sorption of 0.15/0.85 CO<sub>2</sub>/N<sub>2</sub> mixture on K-promoted hydrotalcite beads at 623 K and 134 kPa (P<sub>CO2</sub> = 20 kPa) from cycle 0 to cycle 5.

## Future Perspectives

The number of possible “steps” in the cyclic adsorption processes is one of the key parameters to design a highly efficient adsorption process, while it does not have a broad range, accordingly, developing an algorithm for automatic generation of PSA cycles and tuning the various steps can be so helpful in this area. The choice of the best adsorbent material is also one of the main challenges in this topic, that should be addressed.

## Related Sustainable Development Goals



### Outputs

#### Ph.D. Dissertations

[1] Mohsen Karimi, Process Development for Carbon Dioxide Capture Using Novel Adsorbents: Applications for Clean Energy and Environmental Protection, PDEQB, FEUP, 2023.

#### Selected Publications

- [1] Donglei Qu *et al.*, Adsorption 24, 357–369 (2018)
- [2] M. Karimi *et al.*, Chem Eng Technology 43, 1336-1349 (2020)
- [3] M. Karimi *et al.*, J. Env. Chem. Eng. 8, 104069 (2020)
- [4] A. Freire *et al.*, J. Cleaner Prod. 273, 122917 (2021)
- [5] T. J. Lopes *et al.*, Adsorption 27, 1237–1250 (2021)
- [6] M.J. Regufe *et al.*, Energies 14, 2406 (2021)
- [7] M. Karimi *et al.*, Measurement 183, 109857 (2021)
- [8] L. F. A. S. Zafaneli *et al.*, Micro Meso Mater 335, 111818 (2022)
- [9] M. Karimi *et al.*, J. CO<sub>2</sub> Utilization 57, 101890 (2022)
- [10] V. Martins *et al.*, Chem. Eng. Journal 434, 134704 (2022)
- [11] M. Karimi *et al.*, Env. Chem. Letters 21 (2023)

### Team

Alírio E. Rodrigues, Emeritus Professor; Alexandre Ferreira, Assistant Professor / Group Leader; Ana Mafalda Ribeiro, Assistant Professor; Maria João Regufe, PostDoc Researcher; Jonathan Gonçalves, PostDoc Researcher; Mohsen Karimi, Ph.D. Student.

### Funding

LSRE-LCM Base Funding, UIDB/50020/2020, 2020-2023  
 LSRE-LCM Programmatic Funding, UIDP/50020/2020, 2020-2023  
 LA LSRE-LCM Funding, UID/EQU/50020/2019, 2019  
 LA LSRE-LCM Funding, POCI-01-0145-FEDER-006984, 2013-2018  
 Project NORTE-01-0145-FEDER-000006  
 Project VALORCOMP, 0119\_VALOR-COMP\_2\_P, 2014–2020  
 Project HyGreen&LowEmissions NORTE-01-0145-FEDER-000077  
 FCT Scholarships: SFRH/BD/140550/2018

# Cyclic Adsorption Processes

## Gas Phase Separation Processes

### Pressure Swing Adsorption: H<sub>2</sub> purification

**KEYWORDS:** Green Hydrogen / Cryogenic fixed bed adsorption / Natural gas grids / Binder-free 13X

In this work, a novel fixed-bed adsorption apparatus was developed and the binder-free zeolite 13X (BF13X) was tested to purify green hydrogen injected into natural gas grids. Green hydrogen can be a key factor in meeting global energy demand while contributing to climate goals. In this way, breakthrough curve experiments were performed to assess the equilibrium and kinetic adsorption for H<sub>2</sub> and CH<sub>4</sub> in BF13X. This work covers the lack of adsorption data and multicomponent breakthrough curves of H<sub>2</sub>/CH<sub>4</sub> at low temperatures (until 195 K) which were not available in the literature. The equilibrium data were modeled by using the dual-site Langmuir isotherm model and the multicomponent breakthrough curves were simulated using a mathematical model implemented in MATLAB. Performance parameters based on equilibrium data were discussed. Overall, BF13X has great potential to separate H<sub>2</sub> from CH<sub>4</sub> based on equilibrium (higher capacity for CH<sub>4</sub> with fast diffusion of both gases).

#### Introduction

The Green Hydrogen (GH) produced by water electrolysis from renewable sources of energy (e.g., wind, solar, and hydroelectricity) is free of carbon emissions, which can be a key factor in achieving climate goals, since it can replace fossil fuel in the mobility sector, for example. As the interest in GH grows, the development of its distribution network is a hot topic in the scientific community. One alternative is to inject GH into the existing natural gas (NG) pipelines, to avoid new infrastructure investments. One problem concerning the extraction of GH from NG grids relies on the feed concentration that differs very much from the ones of conventional H<sub>2</sub> purification processes (usually H<sub>2</sub> > 70%). In this case, the GH allowed to be injected into the NG grids is limited to 20%. Thus, to improve the conventional purification process, an adsorbent that has an increased capacity of adsorption towards CH<sub>4</sub> is needed, compared to the ones available. To study both the equilibrium and dynamics of sorption in a wide range of temperatures and pressures, a novel cryogenic

Table 1. Dual-site Langmuir isotherm model parameters for CH<sub>4</sub> and H<sub>2</sub> on binder-free zeolite 13X.

Specie	q <sub>m1</sub> mol/kg	q <sub>m2</sub> mol/kg	b <sub>1</sub> kPa <sup>-1</sup>	b <sub>2</sub> kPa <sup>-1</sup>	ΔH <sub>1</sub> kJ/mol	ΔH <sub>2</sub> kJ/mol
CH <sub>4</sub>	2.1	5.1	4.0x10 <sup>-3</sup>	8.0x10 <sup>-2</sup>	-16.1	-18
H <sub>2</sub>	12.7	-	1.6x10 <sup>-4</sup>	-	-7.0	-

fixed-bed adsorption apparatus was developed.

#### Main Scientific Results

In this work, the commercial binder-free beads of zeolite 13X (BF13X) evaluated were kindly provided by Chemiewerk Bad Köstritz GmbH (Germany). The material was manufactured through an advanced synthesis, in which the binder is itself transformed into zeolite matter during the hydrothermal reaction

overcoming the loss in adsorption capacity associated with the binder composite.

The adsorption equilibrium for H<sub>2</sub> and CH<sub>4</sub> was obtained through a breakthrough curves experiment in a novel cryogenic fixed bed adsorption apparatus (Figure 1) specially designed to screen materials at a wide range of temperatures (77 to 333 K) and pressures up to 40 bar. The single and multicomponent breakthrough experiments were performed at 195, 231, and 273 K and pressure up to 18 bar. Figure 2 shows the equilibrium data for H<sub>2</sub> and CH<sub>4</sub> in BF13X and Table 1 summarizes isotherm model parameters.

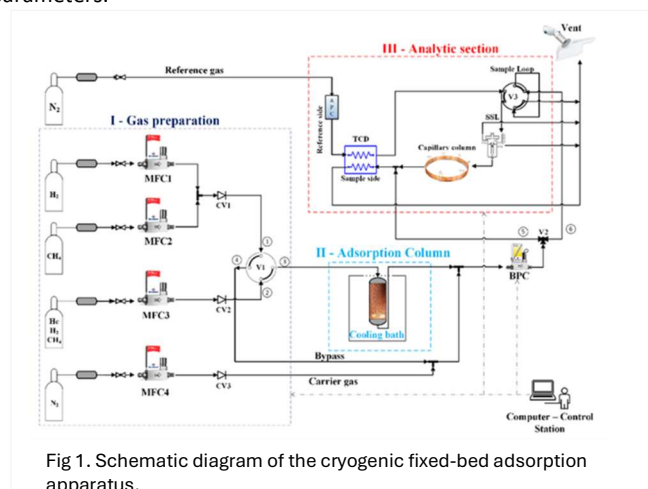


Fig 1. Schematic diagram of the cryogenic fixed-bed adsorption apparatus.

According to the adsorption isotherm in Figure 2, the adsorption capacity for CH<sub>4</sub> on BF13X is significantly higher than for H<sub>2</sub> at the entire experimental conditions. For example, at 195 K and 100 kPa, the loading obtained for CH<sub>4</sub> is 5.20 mol/kg in contrast with 0.17 mol/kg for H<sub>2</sub>, which results in a selectivity of 30 for CH<sub>4</sub> over H<sub>2</sub>. These results indicate that BF13X has excellent potential for the equilibrium separation of H<sub>2</sub> from H<sub>2</sub>/CH<sub>4</sub> by PSA. Lines in Figure 2 show the isotherm model that described very well the experimental data. The loading of CH<sub>4</sub> was found to be 20% higher in BF13X than the zeolite 13X manufactured by conventional pelletization using inert matter. This result points out an opportunity to reduce the CAPEX and OPEX of an industrial unit.

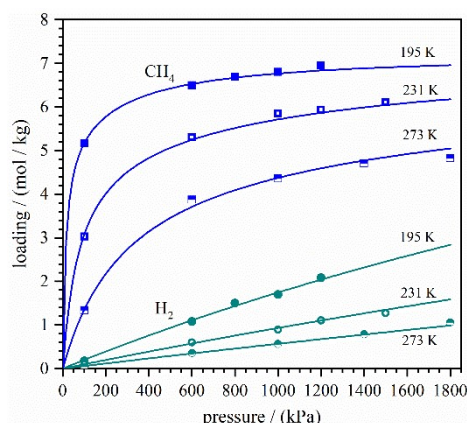


Fig 2. Adsorption equilibrium of H<sub>2</sub> and CH<sub>4</sub> on BF13X. Symbol = experimental; Lines = model.

Figure 3 shows the binary breakthrough curve for a mixture of H<sub>2</sub>/CH<sub>4</sub> (20/80%) in the BF13X at 195 K and 1200 kPa. This experiment starts with a saturated H<sub>2</sub> column. According to Figure 3, it is possible to obtain an H<sub>2</sub>-rich stream (~100 %) in the outlet of the column for approximately 9 min, the time when CH<sub>4</sub> starts to leave the column, which confirms the separation performance of BF13X. The lines in Figure 3 show the mathematical model results that agree very well with the experimental data. The mathematical model was developed based on the mass and energy balances in a fixed-bed adsorption process and was validated in the previous work.

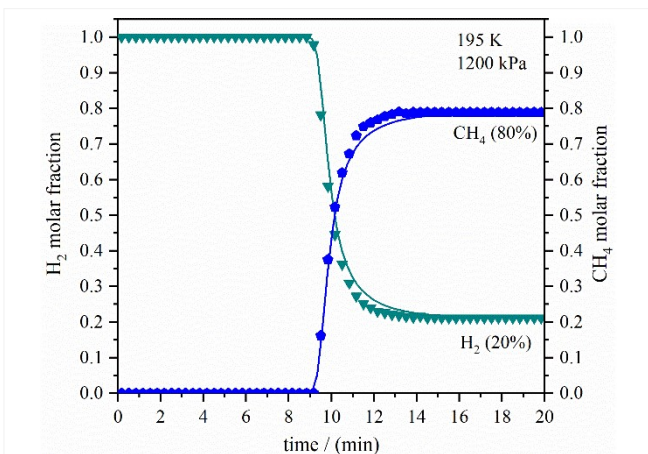


Fig 3. Binary breakthrough curve of CH<sub>4</sub>/H<sub>2</sub> on BF13X at 195 K. Symbol = experimental; Lines = model.

Figure 4 shows the surface plot of the working capacity (WC) estimated taking into account the competitiveness between CH<sub>4</sub> and H<sub>2</sub> to the sites of BF13X by the extended dual-site Langmuir isotherm model. The WC is simply the difference between the loading in the adsorption and desorption conditions. For the adsorption condition, it was considered 4000 kPa and 195 K for a mixture of CH<sub>4</sub>/H<sub>2</sub> (80/20%). In the case of desorption, it was considered a wide range of temperature (195 to 273 K) and pressure (5 to 500 kPa) for the same mixture ratio. Regarding the surface plot in Figure 4, the WC increases as desorption temperature increases and desorption pressure decreases, as expected.

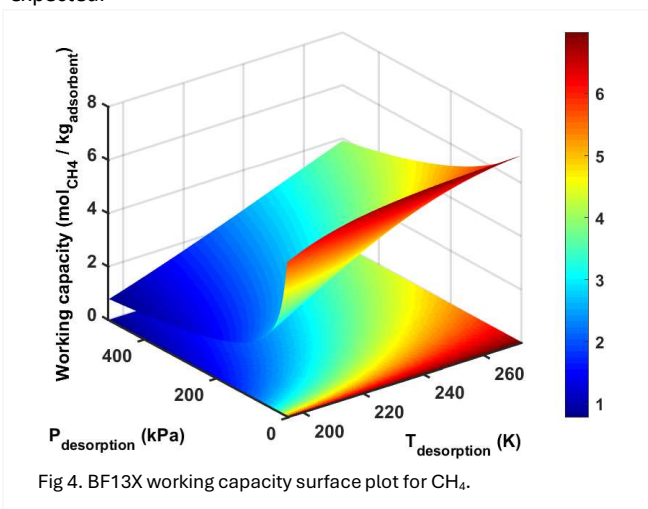


Fig 4. BF13X working capacity surface plot for CH<sub>4</sub>.

A maximum WC of 7.00 mol of CH<sub>4</sub> per kg BF13X is achieved with 5 kPa and 273 K. Note that the desorption pressure has a major impact on the WC since it changes exponentially the WC. In contrast, the changing of desorption temperature seems to have a smooth linear trend on WC. This observation points out that BF13X is suitable to be used in the pressure swing adsorption process which works cyclically by rapidly changing the pressure between adsorption and desorption steps to obtain high performance of production and regeneration.

Overall, this work covers the lack of equilibrium data for CH<sub>4</sub> and H<sub>2</sub> at low temperatures (until 195 K) obtained through breakthrough curve experiments. Moreover, it was shown that the binder-free zeolite 13X has great potential to purify green hydrogen from natural gas pipelines. The data collected and the models developed are now being used to design a pressure swing adsorption process.

### Future Perspectives

As the interest and demand for Green Hydrogen continue to rise, the Pressure Swing Adsorption process exhibits great potential for the recovery of Green Hydrogen from Natural Gas Grids. The Cyclic Adsorption Processes group will persist in exploring and studying new adsorbents and PSA cycle designs to meet hydrogen demands.

### Related Sustainable Development Goals



### Outputs

#### Selected Publications

- [1] L.F.A.S Zafanelli *et al.*, Separation and Purification Technology 307, 122824 (2023)
- [2] S. Jamali *et al.*, Adsorption 24, 481–498 (2018)

#### Team

Alírio E. Rodrigues, Emeritus Professor; Adriano Henrique, PostDoc Researcher; Lucas F. A. S. Zafanelli, Ph.D. Student

#### Funding

PTDC/EQU-EPQ/0467/2020, 2021-2023  
 LSRE-LCM Base Funding, UIDB/50020/2020, 2020-2023  
 LSRE-LCM Programmatic Funding, UIDP/50020/2020, 2020-2023  
 LA LSRE-LCM Funding, UID/EQU/50020/2019, 2019  
 LA LSRE-LCM Funding, POCI-01-0145-FEDER-006984, 2013-2018  
 FCT Scholarships: SFRH/BD/7925/2020

# Cyclic Adsorption Processes

## Gas Phase Separation Processes

### Pressure Swing Adsorption: Light Hydrocarbons Separation

**KEYWORDS:** Adsorption / Separation / Olefins / Paraffins / Pressure Swing Adsorption / Particle Swarm Optimization

Vacuum Pressure Swing Adsorption processes were developed and validated for the separation of ethane/ethylene mixtures using a  $\text{Cu}(\text{Qc})_2$  Metal Organic Framework (MOF) adsorbent, and separation of ethane/propane and ethylene/propane mixtures using MIL-100(Fe) MOF. Adsorption equilibrium and kinetic properties were experimentally measured by gravimetric methods and breakthrough experiments. Lab-scale VPSA processes were designed and experimentally validated. Particle Swarm Optimization algorithms were used to optimize the VPSA operating conditions.

#### Introduction

Ethylene, with 60% consumption in the petrochemical industry, is a building block for synthesizing various petrochemical products, including resins, plastics, and other organic chemicals. In 2017, worldwide ethylene consumption was approximately 150 million tons annually and is expected to reach more than 200 million tons annually by 2023. It can be produced in various grades depending on the final application, but some impurities can affect the properties and performance of the end products; therefore, ethylene should be purified to polymer-grade purity (greater than 99.5 mol%).

Conventionally, cryogenic distillation is the technology employed to produce polymer-grade ethylene (>99.9%) from ethane/ethylene mixtures and is one of the most challenging and energy-consuming separation practices at the industrial level. This is a highly demanding process from energy and economic points of view, and many studies aim to find technological solutions to substitute the conventional process for more sustainable alternatives. Among the competing alternatives toward this end, cyclic adsorption processes such as pressure swing adsorption (PSA), and simulated moving bed (SMB) technologies appear to be the most promising and energy-efficient options.

Several studies have been carried out by the group to separate ethane/ethylene mixtures in gas-phase by SMB technology, mainly using propane as desorbent. In this case study, propane must be recovered from the extract and raffinate streams by two additional separations: ethylene/propane (extract) and ethane/propane (raffinate). The main objective of this work is to propose PSA cycles to perform the SMB downstream separations and to show that this process can be an efficient alternative. Figure 1 summarizes the outline of this case study. However, in adsorption processes, the adsorbent has an impact on the final process performance. To achieve high performance, it is also necessary to take into account the selectivity, working capacity, adsorption affinity, and regeneration capacity of the adsorbent. For this case study, MIL-100(Fe) emerged as a potential candidate for the selective adsorption of propane over ethane and ethylene, based on the results available in the literature to separate hydrocarbon mixtures by carbon number—C3/C4 mixtures, together with the available adsorption equilibrium data for this material. This case study aims

Another approach for the ethylene/ethane separation considers the use of paraffin selective adsorbents. These adsorbents are efficient for PSA because they can directly recover high-purity ethylene in a single adsorption step under high adsorption pressure and atmospheric temperature.

Additionally, because the ethane fraction in the C2 splitter feed was approximately 10–20 mol%, the amount of adsorbent and vacuum pump load could be reduced. The second case study aims to separate ethane and ethylene using vacuum pressure swing adsorption on a  $\text{Cu}(\text{Qc})_2$  metal-organic framework (MOF) adsorbent. Also, the target is to obtain polymer grade, i.e., over 99.6 mol% ethylene purity with maximum ethylene recovery and productivity.

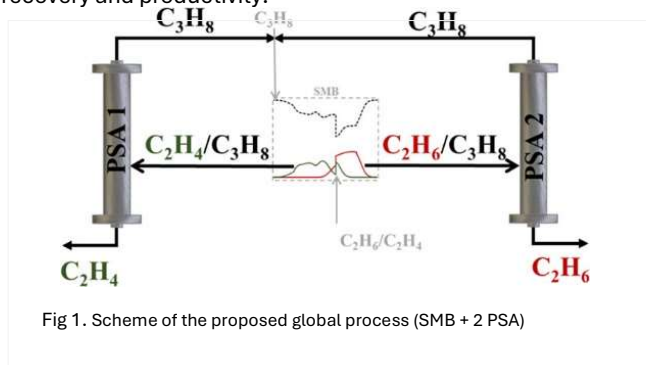


Fig 1. Scheme of the proposed global process (SMB + 2 PSA)

#### Current Development

Single adsorption equilibrium isotherms of ethane, ethylene, and propane over MIL-100(Fe) in granule form were measured by a gravimetric method. MIL-100(Fe) presented a higher adsorption capacity for propane when compared with ethane and ethylene. The Dual-Site Langmuir model describes well the heterogeneity of the adsorbent surface for all three compounds. The amount of ethane, ethylene, and propane adsorbed decreases with increasing temperature; however, the preferential adsorption of propane toward C<sub>2</sub> compounds does not change with temperature.

The heat of adsorption at zero coverage for the three compounds in the study was calculated, and the values showed that propane has the strongest interaction with the adsorbent, corroborating all the information collected from the equilibrium studies.

The working capacities and selectivity parameters for MIL-100(Fe) granules at three different temperatures and different regeneration pressures showed that the regeneration process could be performed at 50 kPa.

The ideal selectivity at 323 K showed higher values for low pressure, and above 200 kPa remains practically constant. The ideal selectivity does not change significantly with temperature and pressure, except for 323 K, for which for pressures up to 200 kPa the selectivity is around 4 and then decreases, achieving selectivity close to 2 at 750 kPa. The selectivity values suggest that the separation of C<sub>3</sub>/C<sub>2</sub> over MIL-100(Fe) granules using PSA might be undemanding.

The single breakthrough curves were measured at 323 K and 150 kPa and showed the same tendency in the adsorption capacity, already observed in the equilibrium. That is, propane breaks at 750 s, and is the one with the highest adsorption capacity, since ethane and ethylene break at 295 and 280 s, respectively.

From the multicomponent curves measured, it is possible to observe that propane is capable of displacing ethane and ethylene from MIL-100(Fe). The mathematical model employed not only predicts well the experimental results for the pure

components but it also describes the experimental multicomponent data accurately.

Additionally, in this work, PSA technology at the bench scale was evaluated for propane recovery and to produce ethylene and ethane from 0.30 ethane/0.70 propane and 0.30 ethylene/0.70 propane mixtures using MIL-100(Fe), to separate the extract and raffinate streams from an SMB separation unit.

The VPSA cycles proposed are composed of five steps, with two different feed compositions, 0.30 ethane/0.70 propane and 0.30 ethylene/0.70 propane, at 323 K and 150 kPa on MIL-100(Fe). For cycle scheme 1, an ethane purity of 99.5% was attained with a productivity of  $1.7 \text{ mol}_{\text{C}_2\text{H}_6} \cdot \text{h}^{-1} \cdot \text{kg}^{-1}$ , and with a reasonable ethane recovery (86.7%). In the same cycle, 99.4% of propane is recovered with 97.0% purity and a productivity of  $4.5 \text{ mol}_{\text{C}_3\text{H}_8} \cdot \text{h}^{-1} \cdot \text{kg}^{-1}$ . In cycle scheme 2, an ethylene purity of 100.0% was achieved with a productivity of  $1.4 \text{ mol}_{\text{C}_2\text{H}_4} \cdot \text{h}^{-1} \cdot \text{kg}^{-1}$ , with a moderate ethylene recovery of 75.8%. The propane was recovered in full with a purity of 94.7% and a high productivity of  $4.3 \text{ mol}_{\text{C}_3\text{H}_8} \cdot \text{h}^{-1} \cdot \text{kg}^{-1}$ , also in cycle scheme 2. The results show that this technology is very promising to be implemented for this type of separation on a large scale. Additionally, a power consumption of 891 Wh/kg<sub>C<sub>3</sub>H<sub>8</sub></sub> and 849 Wh/kg<sub>C<sub>3</sub>H<sub>8</sub></sub> was calculated for the ethane/propane and ethylene/propane separations. These values are normalized by the amount of propane produced.

The experimental results are in good agreement with the results obtained by simulation considering the complete model. The model validation with experimental results, of bench-scale experiments, is of utmost importance since it allows the industrial design of a process of higher dimensions, as well as its further optimization.

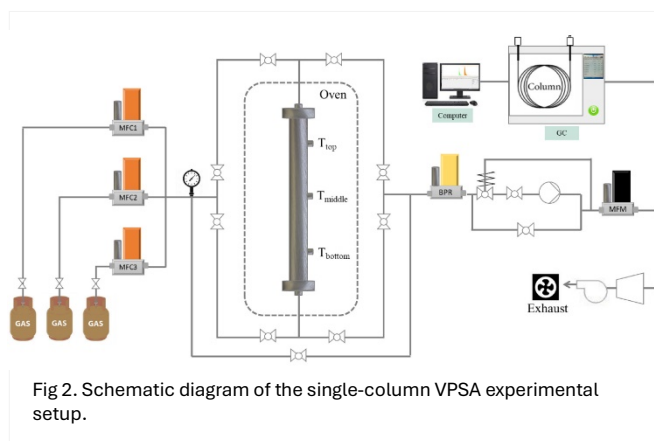


Fig 2. Schematic diagram of the single-column VPSA experimental setup.

In collaboration with the Korea Research Institute of Chemical Technology (KRICT), a VPSA process was developed to purify the ethylene from ethane/ethylene mixtures using the Cu(Qc)<sub>2</sub> MOF adsorbent. A Cu(Qc)<sub>2</sub> MOF adsorbent was synthesized and granulated. The adsorption isotherms and breakthrough curves were measured using a granulated adsorbent. A numerical simulation model for adsorption was developed. The Quadratic-Langmuir isotherm predicted the equilibrium data well. Based on the validation of experiments and simulation of single and binary breakthrough curves, the LDF mass-transfer coefficients of ethane and ethylene were approximately  $0.1 \text{ s}^{-1}$  and  $1.01 \text{ s}^{-1}$ , respectively. Based on the Length of Unused Bed study, the feed flow rates for the pressurization and adsorption steps were determined to be 0.03 SLPM. The VPSA process was designed as a two-bed, five-step process consisting of the pressurization, adsorption, rinse, blowdown, and purge steps. Under nominal operating conditions, ethylene productivity, purity, and recovery were  $1.84 \text{ mol/kg/hr}$ , 99.68 mol%, and 65.28%, respectively. Sensitivity analysis was conducted with six operating variables that had the greatest influence on the VPSA results. The time

and flow rate of the rinse step had the highest influence on the purity and recovery of ethylene. Particle Swarm Optimization was applied to optimize ethylene recovery from nominal VPSA with a purity constraint. The optimized VPSA process showed a productivity of  $1.98 \text{ mol/kg/hr}$ , and a purity and recovery of 99.60 mol% and 76.57%, respectively. The productivity and recovery of ethylene were improved by 11.29% and 0.14 mol/kg/hr, which showed that the VPSA process using the

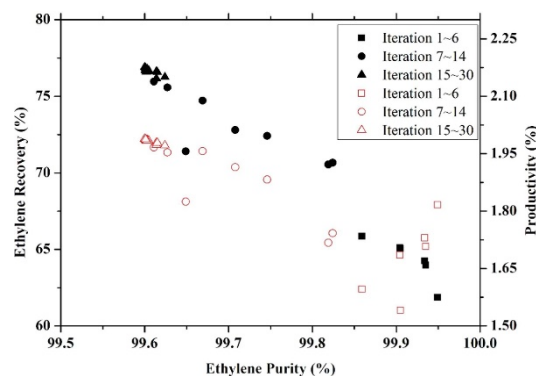


Fig 3. Optimization results of different iteration step of PSO. The marker represents an optimum particle of each iteration (black: ethylene recovery; red: productivity).

Cu(Qc)<sub>2</sub> MOF adsorbent could be a viable option to the conventional C<sub>2</sub> splitter distillation.

#### Future Perspectives

The results obtained reveal that cyclic adsorptive processes are a viable, competitive alternative to the currently used cryogenic distillation process. Additionally, the current results show this way, LSRE activities will continue in this area exploring potential new adsorbents and/or new designs to respond to relevant industrial problems separations.

#### Related Sustainable Development Goals



#### Outputs

#### Selected Publications

- [1] V.F. Martins *et al.*, Ind. Eng. Chem. Res. 59, 10568 (2020)  
[2] J.S. Yun *et al.*, Sep. Purif. Technol. 326, 124711 (2023)

#### Team

**Alírio E. Rodrigues** Emeritus Professor; José M. Loureiro Associated Professor; Alexandre Ferriera, Assistant Professor / Group Leader; **Ana M. Ribeiro**, Assistant Professor; **Paulo Carmo**, Junior Researcher; **Vanessa F.D. Martins**, Ph.D. student; **Rute Seabra**, Ph.D. Student; **Paulo Silva**, M.Sc. Student

#### Funding

LSRE-LCM Base Funding, UIDB/50020/2020, 2020-2023  
LSRE-LCM Programmatic Funding, UIDP/50020/2020, 2020-2023  
LA LSRE-LCM Funding, UID/EQU/50020/2019, 2019  
LA LSRE-LCM Funding, POCI-01-0145-FEDER-006984, 2013-2018  
ALICE, LA/P/0045/2020, 2020  
NORTE 2020, NORTE-01-0145-FEDER-000006, 2020

# Cyclic Adsorption Processes

## Gas Phase Separation Processes

### Pressure Swing Adsorption: Hexane Isomers Separation

**KEYWORDS:** RON improvement of gasoline; Metal-organic frameworks; Zeolites; Activated Carbons

In this research, a new adsorptive process regarding the separation of pentane and hexane isomers, to recover high RON paraffins from light naphtha fractions was developed, which led to an experimentally and unprecedented final product with a 92 RON ideal productivity of  $1.14 \text{ mol.dm}^{-3}$ . The core of the innovative technology with considerable potential for the refining industry relies on the complementary role played by the MOF MIL-160(Al) and the benchmark zeolite 5A integrated into a mixed-bed adsorber. Furthermore, resorcinol-formaldehyde aerogel and xerogel were tested as selective adsorbents of hexane isomers under static and dynamic conditions. This work aims to further study the carbon molecular sieve behavior of some of these samples for linear and branched hydrocarbon separation in the gas phase, and the possibility of tuning the adsorptive properties of the xerogel using physical activation with carbon dioxide.

#### Introduction and Objectives

The production of high-quality gasoline is currently achieved through the energy-demanding conventional Total Isomerization Process (TIP) that separates pentane and hexane isomers while not reaching yet the ultimate goal of a Research Octane Number (RON) higher than 92. Herein we demonstrate how an unprecedented synergistic action of two complementary benchmark materials of each family of porous solids, a commercially available zeolite, 5A and the bio-derived Al-dicarboxylate MOF MIL-160(Al), leads to a novel adsorptive process for octane upgrading of gasoline through an efficient separation of pentane and hexane isomer mixtures into fractions of low and high research octane number (LRON/HRON). This innovative mixed bed adsorbent strategy encompasses a thermodynamically-driven separation of hexane isomers according to the degree of branching by MIL-160(Al) coupled to a steric rejection of pentane and hexane linear isomers by the molecular sieve zeolite 5A. The adsorptive separation ability of this MOF/zeolite duo was further evaluated under industrial operating conditions by sorption breakthrough and continuous cyclic experiments with a mixed bed of shaped adsorbents. Remarkably, at the industrially relevant temperature of 423 K, an ideal sorption hierarchy of low RON over high RON alkanes is achieved, *i.e.*, n-hexane  $\gg$  n-pentane  $\gg$  2-methylpentane  $>$  3-methylpentane  $\gg\gg$  2,3-dimethylbutane  $>$  isopentane  $\approx$  2,2-dimethylbutane, and exceptional ideal productivity of  $1.14 \text{ mol.dm}^{-3}$  is attained for a final high RON isomers product of 92, which corresponds to a substantial leap-forward when compared with existing processes.

Furthermore, a carbon aerogel and a series of physically activated carbon xerogels were tested as adsorbents of the  $C_6$  alkane isomers under static and dynamic conditions. Adsorption capacities for the different compounds were explained according to material porosity. The influence of the drying conditions and the physical activation with carbon dioxide on porosity, and consequently, on the adsorptive behavior of samples was also evaluated.

#### Current Development

The separation of the alkanes was evidenced by experimental breakthrough data collected for the mixed bed of 70 wt% MIL-160(Al) (shaped beads of 2.0 to 3.35 mm) and 30 wt% zeolite 5A (binder-free beads of 1.2 to 2.0 mm) at industrially relevant separation conditions (423 K and 50 kPa of total isomers pressure), which demonstrates the desired fractioning between fractions of HRON (22DMB, 23DMB and i-C5), and LRON (n-C6, n-C5, 2MP and 3MP) isomers. Fig. 1 reveals such data with an ideal sorption hierarchy: n-C6  $\gg$  n-C5  $\gg$  2MP  $\approx$  3MP  $\gg\gg$  23DMB  $>$  i-C5  $\approx$  22DMB associated with an excellent productivity of  $1.14 \text{ mol.dm}^3$  for a RON of 92.

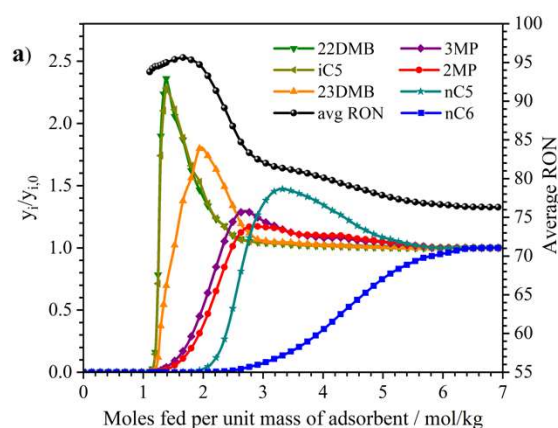


Fig. 1 - Separation of all pentane and hexane isomers by MIL-160(Al) and Zeolite 5A mixed bed adsorbent. Breakthrough data for an equimolar mixture feed in the mixed fixed bed at 423 K and total isomers pressure of 50 kPa

Also, preliminary cyclic PSA experiments were carried out with all pentane and hexane isomers mixture to prove that the MIL-160(Al)/Zeolite 5A duo can be effective in upgrading the actual TIP process under continuous cyclic adsorption operation. Fig. 2 shows the Cyclic Steady State (CSS) of a simplified 2-step PSA experiment, *i.e.*, (i) pressurization and adsorption with feed and (ii) vacuum countercurrent depressurization with inert He purge (desorption). This experiment revealed that at step I (adsorption), the mass front of the HRON 22DMB and i-C5 has completely left the column, while the mass transfer front of 23DMB is concentrated at the exit of the column. The mass transfer front of the other LRON isomers mostly remains inside of the bed. Decisively, this PSA experiment confirms the viability of the novel mixed bed adsorbent to separate all pentane and hexane isomers in continuous cyclic operation into distinct HRON and LRON fractions.

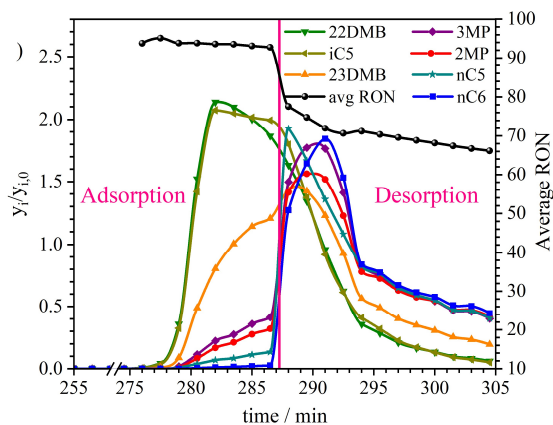


Fig.2 - Separation of all pentane and hexane isomers by MIL-160(Al) and Zeolite 5A mixed bed adsorbent. Cyclic Steady State conditions of a PSA experiment. Adsorption, Step I- Pressurization and feed; Desorption, Step II - Vacuum countercurrent depressurization followed by inert He purge

Regarding the activated carbon samples, differences in textural properties depending on the drying process affected the adsorption of the different hexane isomers, being the aerogel AC16 with narrower micropores but larger micropore volume, much more selective for n-hexane adsorption than the xerogel AC16X with wider micropores and shorter micropore volume. Activation of the carbon xerogel produced new micropores at low burn-off in the sample AC16X10 while micropore widening occurred when it was further activated to obtain the adsorbent AC16X40 with the expected consequences for the linear to branched adsorption selectivity. All of the samples contain a large mesopore volume (xerogels) or macropore one (aerogel) so, even though regeneration was not tested, it should be feasible at mild conditions. These behaviors were proven by competitive adsorption of both hydrocarbons under dynamic conditions, where the aerogel AC16 exhibited excellent behavior as a carbon molecular sieve to separate n-hexane and 2,2'-DMB in the gas phase, as observed in Figure 3. The sample AC16X10 was also able to separate both isomers, but in this case, the difference between both breakthrough times was shortened. Finally, both breakthrough times became almost equal when AC16X40 was employed. Regarding the possibility of their industrial application (cost and scale up), aerogel could be the more problematic because of the need for supercritical drying equipment at a large scale. Nevertheless, its superior performance may well justify the need to include this technique during the synthesis.

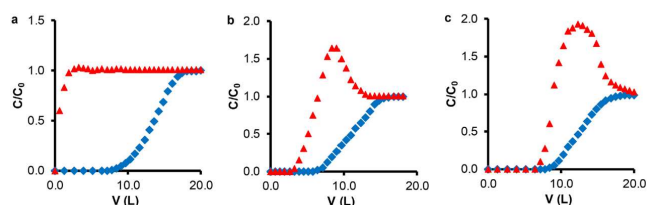


Fig.3 - Breakthrough curves for n-hexane (♦) and 2,2-DMB (▲) competitive adsorption at 30 °C onto a) AC16, b) AC16X10, and c) AC16X40.

### Future Perspectives

We revealed in this research that the integration of a highly stable, bio-derived, and easily scalable green MOF material in its shaped form with a binder-free zeolite 5A resulted in a new advanced recycling pressure swing adsorption (PSA) technology for TIP processes (Fig. 3) that achieves an unprecedented RON higher than 92 for a feed containing all of the pentane and hexane isomers. This ground-breaking process with considerable potential for the refining

industry relies on the complementary role played by the MOF, thermodynamic-separation, and the zeolite, molecular sieving, integrated in the mixed-bed to effectively separate complex pentane and hexane mixtures into HRON (i-C5/23DMB/22DMB) and LRON (n-C5/n-C6/2MP/3MP) fractions.

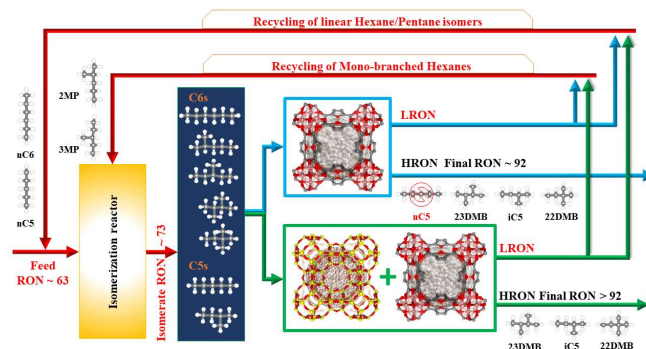


Fig. 3 - Schematic representation of the developed recycling technology for TIP processes. Upgraded TIP process using a mixed adsorption bed of shaped MOF-MIL-160(Al) and binder-free zeolite 5A operating under continuous cycling Pressure Swing Adsorption (PSA) to fractionate the hexane isomers reactor output into a final HRON (>92) isomerate product and a LRON recycle effluent fraction back to the reactor.

### Related Sustainable Development Goals



### Outputs

#### PhD Theses

Adriano Henrique, Upgrading of Total Isomerisation Processes with Metal-Organic Frameworks, 2023. PDEQB/PDEA, FEUP, 2022

#### Patents

Serre *et al.*, USpatent -US 202200081377A1

#### Selected Publications

- [1] J. F. Vivo-Vilches *et al.*, Microporous and Mesoporous Materials 270, 161-167 (2018)
- [2] P. A. P. Mendes *et al.*, Springer Proceedings in Mathematics & Statistics 224, 257-271(2018)
- [3] A. Henrique *et al.*, Ind. Eng. Chem. Res. 58, 378-394 (2019)
- [4] A. Henrique *et al.*, Separation and Purification Technology 238, 116419 (2020)
- [5] A. Henrique *et al.*, J. Mater. Chem. A, 8, 17780-17789 (2020)
- [6] Brântuas P. *et al.*, Advanced Science, 9 (2022)
- [7] Henrique A. *et al.*, Chemical Engineering Journal 472, 145138 (2023)

#### Team

**Alúrio E. Rodrigues**, Emeritus Professor; Alexandre Ferreira, Assitant Professor / Group Leader; Ana Mafalda Ribeiro, Assistant Professor; Pedro Brântuas, PostDoc Researcher; Adriano Henrique, *Ph.D.* Student; Jose F. Vivo-Vilches, Visiting *Ph.D.* Student; Christophe Siquet, Project Researcher

### Funding

Upgrading of Total Isomerization Processes with Metal-Organic Frameworks; PTDC/REQ-PRS/3599/2014  
 LSRE-LCM Base Funding, UIDB/50020/2020, 2020-2023  
 LSRE-LCM Programmatic Funding, UIDP/50020/2020, 2020-2023  
 LA LSRE-LCM Funding, UID/EQU/50020/2019, 2019  
 LA LSRE-LCM Funding, POCI-01-0145-FEDER-006984, 2013-2018  
 CIMO, UID/AGR/00690/2020  
 FCT Scholarships: SFRH/BD/148525/2019

# Cyclic Adsorption Processes

## Gas Phase Separation Processes

### Temperature/Pressure Swing Adsorption: Monomers Recovery

**KEYWORDS:** Ethylene / Propylene / Vinyl Chloride / Adsorption / Separation / Environment / PSA / TPSA / Multitubular TPSA

Eleven Multitubular Temperature/Pressure Swing Adsorption systems were developed for the recovery of unreacted monomer/nitrogen mixtures from polyethylene, polypropylene, and polyvinyl chloride industries. Adsorption equilibrium and kinetic properties were determined for two activated carbons, Maxsorb and Carbotech, and for MIL-100(Fe) MOF. High-purity monomer streams and nitrogen streams fit for open-air release were produced, bypassing the need for incineration. For the recovery of vinyl chloride, a MIL-100(Fe) PSA system achieved an electrical energy consumption of  $0.83 \text{ MJ/kg}_{VCM}$ , while a Maxsorb MT-TPSA system achieved a productivity of  $8.41 \text{ mol/kg}_{ads}h$ . For the recovery of ethylene, a MIL-100(Fe) PSA system is recommended. For the recovery of propylene, both a MIL-100(Fe) PSA and MT-TPSA system can be considered.

#### Introduction

The most common thermoplastic materials are polyethylene, polypropylene, and poly(vinyl chloride), created by a polymerization reaction from the respective monomers: ethylene, propylene, and vinyl chloride. The polymerization reaction for each monomer can be performed through different processes to create polymers with diverse characteristics and applications. However, depending on the process and the monomer used, a percentage of unreacted monomer will remain in the final polymer. The monomer is purged from the polymer by using a degassing system. Indeed, the polymer is blown to atmospheric pressure and then stripped with a hot inert gas, commonly nitrogen. Together, with the emissions from the reactor vent and other equipment purges, the polymer degassing streams have a typical composition of approximately 30:70 % (v/v) monomer/nitrogen. For polyethylene and polypropylene, unreacted monomer accounts for 1 to 2 % (v/v) of the feedstock. For poly(vinyl chloride), this percentage can increase from 10 to 15 % (v/v). In many plants, either due to quality or environmental and health concerns, these vent streams are sent to a flare for incineration. However, these losses could amount from 2000 to 4000 tonnes of monomer a year; incineration is economically disadvantageous and heavily contributes to increasing the plastic industry's carbon footprint. As such, the development of monomer recovery technologies has always been significantly incentivized.

The main objective of this topic is to study and develop adsorption-based separation processes for monomer recovery in nitrogen-rich streams from the top-producing polymer industries. This unit must be capable of producing a stream heavy on the monomer, with a high enough purity to be recycled back into the polymerization reactor, and a nitrogen-heavy stream with a monomer content inferior to the respective atmospheric emission limit. (Figure 1) The applicability of the developed Pressure Swing Adsorption (PSA), Temperature Pressure Swing Adsorption (TPSA), and Multitubular Temperature Pressure Swing Adsorption (MT-TPSA) cyclic processes in an industrial setting will be discussed and compared to the existing solutions. The adsorption performance of the MOF material MIL-100(Fe) will be tested for the separation of ethylene, propylene, and vinyl chloride in nitrogen mixtures. The separation performance of the Pittsburgh, Maxsorb, and Carbotech activated carbons will be

investigated solely for the separation of vinyl chloride and nitrogen.

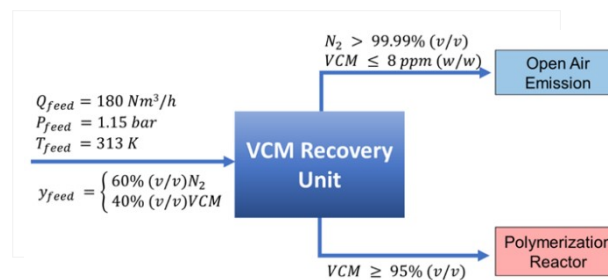


Fig 1. Separation Specifications and Block Flow Diagram of the proposed VCM recovery unit

#### Current Development

In the reported period, a total of eleven adsorption-based processes have successfully been proposed to control and recover unreacted monomers in nitrogen-rich gas vent streams in poly(vinyl chloride), polyethylene, and polypropylene industries. More specifically, the developed separation units must have the ability to control the monomer concentration on process units' vent streams, to below the OSHA standards of gaseous exhaust streams (8 ppm(w/w) for vinyl chloride, and 20 ppm (v/v) for light olefins). They must be capable of producing a 95 % (v/v) monomer purity stream to be recycled into the polymerization process.

Adsorption equilibrium data for vinyl chloride, ethylene, propylene, and nitrogen was successfully measured using gravimetric methods on MIL-100(Fe), activated at 433 K.

Single, binary, and pseudo-binary breakthrough experiments were performed on a bench-scale single column PSA unit and were successfully simulated using the developed fixed bed mathematical model for the ethylene/nitrogen and propylene/nitrogen mixtures in MIL-100(Fe).

For the recovery of vinyl chloride, preliminary testing was performed using Pittsburgh PCB activated carbon to ascertain the viability of standard cyclic adsorption separation systems using equilibrium data found in the literature. From this research, a TPSA and a MT-TPSA cycle was successfully designed using a one- and two-dimensional fixed bed models. In turn, an equivalent one-dimensional model was proposed to simulate the radial thermal behavior of temperature-intensive adsorption processes and save on computational time and resources. The developed 7-step, 2-column TPSA operates between a 0.5 to 1 bar and 293 to 463 K range and requires 6225 kg of Pittsburgh PCB carbon. A VCM productivity of  $0.46 \text{ mol/kg}_{ads}h$  was obtained for total thermal energy consumption of  $3.62 \text{ MJ/kg}_{VCM}$ . The proposed 6-step, 3-MTA unit follows a MT-TPSA cycle operated in a 0.5 to 1 bar and 293 to 393 K range and requires total adsorbent load of 1350 kg. A productivity and recovery capacity of  $2.35 \text{ mol/kg}_{ads}h$  and  $24.35 \text{ kg}_{VCM}/(\text{m}^3_{unit}h)$  were obtained for total thermal energy consumption of  $4.88 \text{ MJ/kg}_{VCM}$ .

From the experimental equilibrium and dynamic results obtained, the following adsorption-based separation systems were developed for the recovery of vinyl chloride:

A six-step two multitubular adsorber (MTA) system was developed using commercial Maxsorb carbon. The proposed

system reports productivity of 8.41 mol/(kg<sub>ads</sub>.h) or 69 kg<sub>VCM</sub>/(m<sup>3</sup><sub>unit</sub>.h), a total adsorbent load of 367 kg, with a total thermal energy consumption of 3.05 MJ/kg<sub>VCM</sub>, of which 1.82 MJ/kg<sub>VCM</sub> are necessary to supply thermal energy during the heating and cooling stages.

Using Carbotech carbon, two case studies were considered. The first case study considers the implementation of an adsorptive separation process as the primary separation unit. The second case study considers a pre-existing membrane separation system and proposes a hybrid separation system. An MT-TPVSA cycle was successfully designed for each of the two case studies. For the first case, the designed unit requires a total adsorbent load of 724 kg and an average power consumption of 53 kW. A VCM productivity of 4.38 mol/(kg<sub>ads</sub>.h) or 60.19 kg<sub>VCM</sub>/(m<sup>3</sup><sub>unit</sub>.h) was achieved for a total energy consumption of 3.21 MJ/kg<sub>VCM</sub>. For the second case, proposed separation unit requires a total adsorbent inventory of 24 kg and average power consumption of 1.2 KW in addition to the membrane system. A VCM productivity of 1.96 mol/(kg<sub>ads</sub>.h) or 16.82 kg<sub>VCM</sub>/(m<sup>3</sup><sub>unit</sub>.h) were achieved for a total energy consumption of 4.96 MJ/kg<sub>VCM</sub>.

Taking advantage of the mesoporous structure of the MIL-100(Fe) MOF adsorbent, a 5-step 3-column PSA separation cycle, operated at 343 K and in a pressure range of 0.1 to 7 bar, was successfully developed for a separation previously dominated by temperature-swing processes. The performance of the PSA unit was compared to an MT-TPSA cycle using the same material. The PSA cycle achieved a productivity of 3.52 mol/kg<sub>ads</sub>.h and 71.89 kg<sub>VCM</sub>/m<sup>3</sup><sub>unit</sub>.h for an electrical energy consumption of 0.83 MJ/kg<sub>VCM</sub> and ), with an adsorbent load of 900 kg. The reported 6-step 2-MTA process operates between 1 and 3 bar and 303–393 K range and requires 269 kg of adsorbent. A VCM productivity of 10.70 mol/(kg<sub>ads</sub>.h) and 66.83 kg<sub>VCM</sub>/(m<sup>3</sup><sub>unit</sub>.h) were achieved for total thermal energy consumption of 3.68 MJ/kg<sub>VCM</sub>.

As such, depending on the level of integration of the separation unit into the plants' design, either the MIL-100(Fe) PSA or the Maxsorb MT-TPSA systems can be a potential

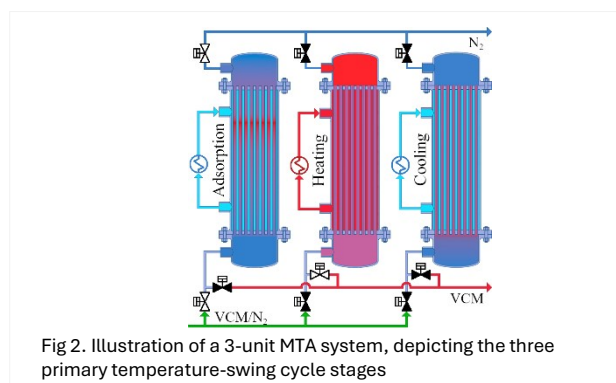


Fig 2. Illustration of a 3-unit MTA system, depicting the three primary temperature-swing cycle stages

solution.

For the recovery of ethylene, a 3-column, 5-step PSA system is recommended. The proposed cycle is operated at a temperature of 343 K and between a pressure range of 0.3 to 9 bar, using a total of 10681 kg of MIL-100(Fe). An ethylene productivity and recovery capacity of 2.23 mol/(kg<sub>ads</sub>.h) and 21.03 kg<sub>C<sub>2</sub>H<sub>4</sub></sub>/(m<sup>3</sup><sub>unit</sub>.h) were achieved for equivalent thermal energy consumption of 10.13 MJ/kg<sub>C<sub>2</sub>H<sub>4</sub></sub>. A 6-step 3-MTA process was also designed for an operating range of 1 to 8 bar and 303 to 393 K, using a total adsorbent mass of 3777 kg. A productivity and recovery capacity of 6.30 mol<sub>C<sub>2</sub>H<sub>4</sub></sub>/(kg<sub>ads</sub>.h) and 24.83 kg<sub>C<sub>2</sub>H<sub>4</sub></sub>/(m<sup>3</sup><sub>unit</sub>.h) was achieved for total thermal energy consumption of 20.81 MJ/kg<sub>C<sub>2</sub>H<sub>4</sub></sub>.

A potential PSA and an MT-TPSA system are suggested for propylene recovery, depending on the integrating process. A 3-column, 5-step PSA cycle, operated at a temperature of 343 K

and in a pressure range of 0.3 to 8 bar, was designed for a MIL-100(Fe) mass of 10681 kg. A propylene productivity and recovery capacity of 1.48 mol<sub>C<sub>3</sub>H<sub>6</sub></sub>/(kg<sub>ads</sub>.h) and 21.03 kg<sub>C<sub>3</sub>H<sub>6</sub></sub>/(m<sup>3</sup><sub>unit</sub>.h) was achieved for a total equivalent thermal energy consumption of 4.37 MJ/kg<sub>C<sub>3</sub>H<sub>6</sub></sub>.

A 3-MTA , 6-step MT-TPSA unit, designed for an operating range of 1 to 5 bar and 303 to 393 K, was designed for a MIL-100(Fe) load of 2359 kg. A propylene productivity and recovery capacity of 6.72 mol<sub>C<sub>3</sub>H<sub>6</sub></sub>/(kg<sub>ads</sub>.h) and 38.91 kg<sub>C<sub>3</sub>H<sub>6</sub></sub>/(m<sup>3</sup><sub>unit</sub>.h) was achieved for total thermal energy consumption of 7.46 MJ/kg<sub>C<sub>3</sub>H<sub>6</sub></sub>, of which 4.65 MJ/kg<sub>C<sub>3</sub>H<sub>6</sub></sub> are necessary to supply thermal energy during the heating stages and electrical power for the operation of the gas and liquid pumps.

### Future Perspectives

Development and application of a Dual Reflux Pressure Swing Adsorption (DR-PSA) model and set-up for adsorbents with more linear shaped isotherms (ethylene/nitrogen in MIL-100(Fe), aimed at significantly reduced energy consumption.

Due to the severe lack of adsorption equilibrium and kinetic experimental data for vinyl chloride, LSRE will continue to explore new potential adsorptive materials for monomer/nitrogen recovery adequate for PSA, TPSA, and DR-PSA systems. Use of the produced experimental data to create and validate a molecular simulation framework for the prediction of equilibrium and kinetic data for the adsorption of monomers in crystalline and amorphous adsorbents.

Development and implementation of a molecular simulation + adsorptive process simulation framework as a tool to evaluate the most efficient adsorbent material and adsorptive separation processes for the complete recovery of unreacted monomers from the polyethylene, polypropylene, and poly(vinyl chloride) industries. The developed framework should sweep a list of crystalline and amorphous adsorbent structures, evaluate the potential of the adsorbent material for a given monomer/nitrogen mixture, and determine the applicability of each adsorption-based separation process. The separation processes accounted for in this framework are the Pressure Swing Adsorption, Temperature Swing Adsorption, and Dual-Reflux Pressure Swing Adsorption cycles.

### Related Sustainable Development Goals



### Outputs

#### PhD Theses

[1] Paulo Miguel Oliveira Cardoso do Carmo, "Separation and Recovery of Monomers in Industrial Streams by Adsorption", PDEQB, FEUP, 2021

#### Selected Publications

- [1] P. Carmo et al., Ind. Eng. Chem. Res. 57, 14223 (2018)
- [2] P. Carmo et al., AIChE Journal 66, e16899 (2019)
- [3] P. Carmo et al., Ind. Eng. Chem. Res. 61, 9433 (2022)
- [4] P. Carmo et al., Fluid Phase Equilib. 562, 113547 (2022)
- [5] P. Carmo et al., Microporous Mesoporous Mater. 352, 112510 (2023)

#### Team

**Alírio E. Rodrigues** Emeritus Professor; **Alexandre F.P. Ferreira** Assitant Professor / Group Leader; **Ana M. Ribeiro** Assitant Professor; **Paulo Carmo** Ph.D. Student.

#### Funding

LSRE-LCM Base Funding, UIDB/50020/2020, 2020-2023  
 LSRE-LCM Programmatic Funding, UIDP/50020/2020, 2020-2023  
 LA LSRE-LCM Funding, UID/EQU/50020/2019, 2019  
 LA LSRE-LCM Funding, POCI-01-0145-FEDER-006984,2013-2018  
 ALICE, LA/P/0045/2020, 2020  
 COMPETE2020, POCI-01-0145-FEDER-006984, 2020  
 NORTE2020, NORTE-01-0145-FEDER-000006, 2020  
 LSRE-LCM – UID/QUE/50020/2019, 2019

FCT

Scholarships:

PD/BD/135063/2017

# Cyclic Adsorption Processes

## Gas Phase Separation Processes

### Temperature Swing Adsorption: Water harvesting

**KEYWORDS:** Water / Air / Adsorption / MIL-125(Ti)\_NH<sub>2</sub> / MIL-160(Al) / MIL-100(Fe) / (P)TSA / Optimization

During the reporting period, various metal-organic framework materials for water harvesting were studied, employing Temperature Swing Adsorption as the fundamental process. Specifically, materials like MIL-125(Ti)\_NH<sub>2</sub>, MIL-160(Al), and MIL-100(Fe) were studied as potential adsorbents for the aforementioned purpose.

#### Introduction

The global challenges of climate change and population growth contribute to the emergence of water stress. The water crisis is one of the main global risks based on its societal impact, particularly the access to safe drinking water in regions with a dry (arid) or mainly dry (semi-arid) climate. The United Nations recognizes access to water and sanitation as human rights, leading to the development of policies and goals aimed at achieving this fundamental objective.

Bringing water from distant locations to arid regions, although a solution, is often costly. Hence, in areas devoid of accessible liquid water sources like arid regions, conflict zones, disaster-stricken areas, or places with heavily contaminated water supplies, atmospheric water content becomes a potential source. Indeed, harvesting water from the air offers drinkable-quality water without spatial constraints and can be powered by renewable energy sources.

Extracting moisture from the atmosphere is possible through Atmospheric Water Vapor Processing (AWVP) technology. This technology can be divided into three categories: Type 1 involves surface cooling using heat pumps or radiative cooling, Type 2 focuses on water vapor concentration using desiccants, and Type 3 relies on convection induced or controlled within a structure.

Various techniques are currently in development. The optimal selection of the extraction method relies on atmospheric and meteorological conditions, along with economic considerations.

Owing to hygroscopic materials' capability to extract and retain water, the efficiency of active dew condensers surpasses that of radiative dew condensers. The most typical active dew condensers involve capturing water using desiccants, which can be in liquid or solid form, employing absorption and adsorption processes.

Regenerative desiccants such as metal-organic frameworks (MOFs) are being explored for water capture through adsorption processes. Indeed, the interest in MOFs for water vapor capture has increased in recent years. Recent publications have confirmed the significant potential of robust MOFs in processes related to water adsorption. These MOFs exhibit stability throughout multiple water adsorption/desorption cycles.

However, the suitability of each MOF/adsorbent for capturing water from the air is contingent upon its adsorption equilibrium isotherm. Therefore, some MOFs/adsorbents are more apt for arid areas, and others are suitable for zones with more humidity – Fig. 1.

While there are numerous studies in the literature evaluating water adsorption equilibria, there is still ample ground to cover, particularly concerning fixed-bed investigations and cyclic adsorption-based studies.

Assessments have already been conducted on the capability of MIL-125(Ti)\_NH<sub>2</sub>, MIL-160(Al), and MIL-100(Fe) to extract

freshwater from the atmosphere through adsorption-desorption processes. All proved to be water-robust and present high capacities for water adsorption even at mild relative humidity, proving their high potential for water harvesting applications. Still, additional research was required to test their ability to be used in a cyclic adsorption-based process. The studies performed during this period aimed to overcome the existing gap in the development of technologies for the cyclic adsorption process for water harvesting, including the study of pressure and temperature swing adsorption processes to do so.

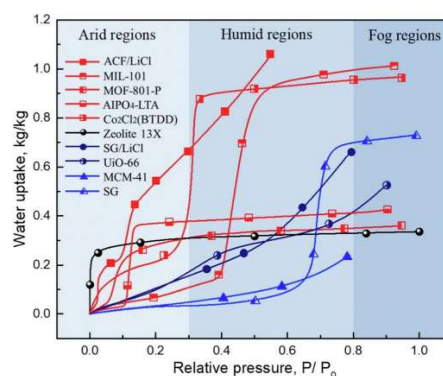


Fig 1. Desiccant materials with high potential for water-harvesting systems in three different scenarios. Image taken from: Tu, Yaodong, et al. "Progress and expectation of atmospheric water harvesting." *Joule* 2.8 (2018): 1452-1475.

#### Current Development

During the reporting period, the water capture potential of MOFs, specifically MIL-125(Ti)\_NH<sub>2</sub>, MIL-160(Al), and MIL-100(Fe) was evaluated.

For MIL-125(Ti)\_NH<sub>2</sub>, adsorption affinity towards different adsorbates (CO<sub>2</sub>, O<sub>2</sub>, N<sub>2</sub>, and H<sub>2</sub>O) and regeneration in adsorption/desorption cycles were examined. Equilibrium isotherms, measured between 283 and 323 K and 0 to 7 bar, revealed Type V isotherms, fitting well with Cooperative Multimolecular Sorption (CMMS) and Polanyi's theory models for water vapor. For the rest of the adsorbates, the Langmuir model was used to fit the experimental data. At P/P<sub>0</sub>=0.83 the material presented a water adsorption capacity of 20.2 mol·kg<sup>-1</sup>. With the Clausius -Clapeyron equation was also possible to estimate the isosteric heat of adsorption for each adsorbate: H<sub>2</sub>O (≈41 kJ·mol<sup>-1</sup>), CO<sub>2</sub> (23.5 kJ·mol<sup>-1</sup>), N<sub>2</sub> (11.5 kJ·mol<sup>-1</sup>), and O<sub>2</sub> (10.0 kJ·mol<sup>-1</sup>). Breakthrough experiments confirmed Type V isotherms (Fig. 2 + 3 a) and Diffuse Reflectance Infrared Fourier Transform Spectroscopy (DRIFTS) showed high adsorbent regeneration capability. The adsorption kinetics demonstrated relatively rapid attainment of equilibrium, typically within around 100 minutes. The proposed pressure-temperature swing adsorption (PTSA) process demonstrated a maximum productivity of 320 L·day<sup>-1</sup>·ton<sup>-1</sup>. The productivity value can possibly be optimized by changing the process parameters.

MIL-160(Al) was also studied for water sorption applications. Adsorption equilibrium isotherms, dynamic adsorption experiments (Fig. 2 +3b)), and MIL-160(Al) granule characterization were conducted. H<sub>2</sub>O vapor adsorption

isotherms at 303, 323, and 343 K presented Type V shapes. CO<sub>2</sub>, N<sub>2</sub>, and O<sub>2</sub> adsorption isotherms revealed CO<sub>2</sub> > O<sub>2</sub> > N<sub>2</sub> affinity. O<sub>2</sub> and N<sub>2</sub> exhibited nearly linear adsorption isotherms, whereas CO<sub>2</sub> demonstrated an isotherm characteristic of the Langmuir type. The CMMS model was used to fit the water vapor experimental data, while for the rest of the gases, the Langmuir model was used. Once again, with Clausius-Clapeyron equation the isosteric heats of adsorption were determined for CO<sub>2</sub> (25.6 kJ·mol<sup>-1</sup>), N<sub>2</sub> (14.1 kJ·mol<sup>-1</sup>), and O<sub>2</sub> (13.6 kJ·mol<sup>-1</sup>). Water vapor breakthrough experiments aligned with water adsorption isotherms, proving water co-adsorption independence from CO<sub>2</sub> and N<sub>2</sub>. DRIFTS confirmed MIL-160(Al) stability. With DRIFTS and TGA it was possible to determine a maximum regeneration temperature rounding 298-423 K, which is quite lower than the thermal stability of the material, which is about 600-650 K. Optimized temperature swing adsorption (TSA) achieved a maximum H<sub>2</sub>O productivity of 305 L·day<sup>-1</sup>·ton<sup>-1</sup>, for a purge temperature of 353 K, condensation temperature of 283 K, and a flowrate of 0.5 m<sup>3</sup>·s<sup>-1</sup>.

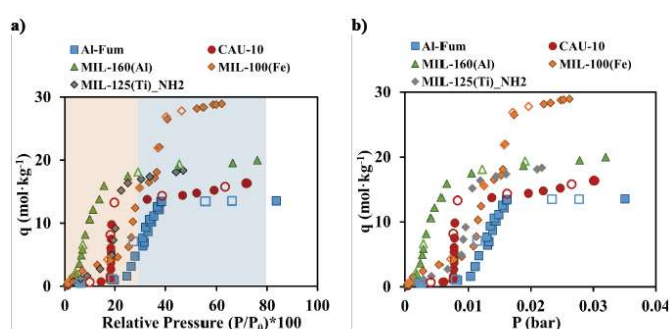


Fig 2. Water vapor adsorption-desorption equilibrium isotherms at 303 K as a function of (a) relative pressure and (b) absolute pressure.

The work developed also investigated the water extraction potential of MIL-100(Fe), assessing its equilibrium and dynamic behavior (Fig. 2 + 3c). CO<sub>2</sub>, N<sub>2</sub>, and O<sub>2</sub> adsorption isotherms showed higher affinity for CO<sub>2</sub>. H<sub>2</sub>O adsorption isotherms followed Type VI isotherms, indicating two-step adsorption (0.21 < P/P<sub>0</sub> < 0.30 and 0.36 < P/P<sub>0</sub> < 0.40) attributed to the presence of two different cavities (25 and 29 Å) on its structure. DRIFTS analysis revealed strong regeneration capability during adsorption/desorption cycles. The TSA process, with a column volume of 0.35 m<sup>3</sup>, achieved a maximum H<sub>2</sub>O productivity of 86.8 L·day<sup>-1</sup>.

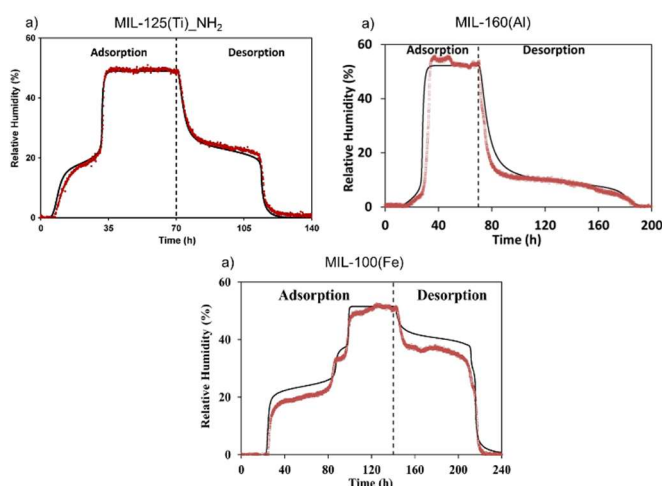


Fig 3. Water vapor adsorption-desorption breakthrough curve obtained at 298 K on a) MIL-125(Ti)\_NH<sub>2</sub>, b) MIL-160(Al) and c) MIL-100(Fe). (Points represent experimental data, full line corresponds to simulation results, and dashed line represents the beginning of the regeneration step).

## Future Perspectives

Other adsorbents that already showed potential for water harvesting can be tested (e.g., super moisture-adsorbent gel (SMAG) and interpenetrating polymer network (IPN), or even the combination of MOFs with other materials). The water harvester's geometry and material can be optimized to enhance heat transfer, thereby reducing heating requirements and achieving a condensation temperature closer to the environmental temperature. Examples include modular beds and tubular solar stills powered by a parabolic concentrator system.

Besides TSA, electric swing adsorption (ESA) can also be explored. To achieve this, hybrid materials with high water adsorption capacity and good electrical conductivity can be developed using extrusion or the more design-flexible technology of 3D printing.

This research work could be the lead-off to the development of a proof-of-concept device for the sorption process and afterward to optimize the efficiency and productivity of the water harvester. When selecting the adsorbent, consideration should be given to the average relative humidity of the location and the most suitable MOF based on local humidity conditions.

## Related Sustainable Development Goals



## Outputs

### PhD Theses

[1] Márcia Patrícia Cardoso da Silva, Water Harvesting by Adsorption Based Processes on MOFs, PDEQB, FEUP, 2021

### Selected Publications

- [1] M. P. Silva *et al.*, Separation and Purification Technology 237, 116336 (2020)  
 [2] M. P. Silva. *et al.*, Adsorption 27, 213-226 (2021)  
 [3] M. P. Silva *et al.*, Separation and Purification Technology 290, 120803 (2022)

## Team

**Alírio E. Rodrigues**, Emeritus Professor; **José Miguel Loureiro**, Associated Professor; **Joaquim L. Faria**, Associated Professor; **Alexandre Ferreira**, Assitant Professor / Group Leader; **Ana Mafalda Ribeiro**, Assitant Professor; **Cláudia G. Silva**, Assistant Professor; **Idelfonso B. R. Nogueira**, PostDoc Researcher; **Márcia P. Silva**, Ph.D. Student.

## Funding

LSRE-LCM Base Funding, UIDB/50020/2020, 2020-2023  
 LSRE-LCM Programmatic Funding, UIDP/50020/2020, 2020-2023  
 LA LSRE-LCM Funding, UID/EQU/50020/2019, 2019  
 LA LSRE-LCM Funding, POCI-01-0145-FEDER-006984,2013-2018  
 FCT Grants: IF/00514/2014

# Cyclic Adsorption Processes

## Gas Phase Separation Processes

### Electric Swing Adsorption: CO<sub>2</sub> Capture

**KEYWORDS:** CO<sub>2</sub> Capture / Monolith / Structured adsorbent / 13X zeolite/ Activated carbon / Materials science / Mixtures / Separation/ Adsorption /3D Printing / Additive Manufacturing / Direct Ink Writing / Electric Swing Adsorption

During the reporting period, various materials for the separation of carbon dioxide and nitrogen were studied, employing Electric Swing Adsorption as the fundamental process. Specifically, materials comprising activated carbons and 13X zeolite were studied to achieve higher carbon dioxide (CO<sub>2</sub>) adsorption capacities while maintaining good electrically conductive properties.

#### Introduction

The Industrial Revolution period was a mark in fossil fuel use as an energy source. Since then, global warming has become a significant issue, and CO<sub>2</sub> emissions are among the principal contributors. In 2022, 89% of greenhouse gas emissions related to energy were attributed to CO<sub>2</sub> emissions from energy combustion and industrial processes. Thus, it is urgent to reduce the CO<sub>2</sub> emissions.

For that, diverse technologies can be applied. The selected technology relies on stream temperature, pressure, and CO<sub>2</sub> concentration, as well as the desired product purity. Typically, the CO<sub>2</sub> capture stage, which includes pre-combustion, post-combustion, and oxy-fuel processes, constitutes 70-80% of the total cost in a full CCS system encompassing capture, transport, and storage. Post-combustion CO<sub>2</sub> capture involves capturing CO<sub>2</sub> from the combustion products or exhaust gases of fossil fuels. Various alternatives, including absorption, membrane separation, hydration, and adsorption, are currently utilized or under study for capturing CO<sub>2</sub>. Among the available technologies, the feasibility of the Electric Swing Adsorption (ESA) process has been tested, and numerous studies have demonstrated its effectiveness for CO<sub>2</sub> capture.

In adsorption processes, the development of new materials is an emerging challenge to increase the CO<sub>2</sub> adsorption capacity of materials and the efficiency of the processes. A literature review on the application of ESA processes for CO<sub>2</sub> capture shows that a relevant number of studies consider hypothetical adsorbents. This is attributed to the challenge of developing materials with ideal characteristics for ESA application, namely high CO<sub>2</sub> adsorption capacity and suitable electrical properties. Thus, in this work, the synthesis of new materials for ESA processes was explored, contributing to advancing knowledge on hybrid materials for ESA. Specifically, the synergy between 13X zeolite (known for high CO<sub>2</sub> adsorption capacity) and activated carbon (recognized for good electrical conductive properties) was investigated.

In addition, the effective shaping of adsorbents is essential to guarantee a high-efficiency energetic process. Extrudates/pellets and monoliths are examples of shaped materials that can be utilized. Extrusion has proven to be an efficient method for producing extrudates/pellets and monoliths. However, it remains crucial to explore different types of monolith structures. Additive manufacturing (3D printing), offers a valuable approach for easily varying monolith geometry. Yet, a primary challenge in utilizing additive manufacturing (AM) is to achieve an ink with the desired adsorbents and suitable rheology for printing. Indeed, there are only a few studies on the preparation of adsorbent materials using 3D printing processes, particularly for CO<sub>2</sub> capture applications involving ESA processes. Here, extrusion and AM

were the methods studied for the development of the hybrid materials.

#### Current Development

In the reporting period, various advanced materials for CO<sub>2</sub> capture processes are explored through different shaping techniques. Extrusion and AM were the technologies used to perform the shaping of the materials.

One approach involves the extrusion process to create a hybrid honeycomb monolith using 13X zeolite (70 wt.) and activated carbon. Single adsorption equilibrium isotherms for carbon dioxide and nitrogen were measured at different temperatures (between 303 and 373 K), and the material exhibited notable carbon dioxide adsorption capacity. The Dual-Site Langmuir (DSL) model was used to fit the experimental data. Additionally, binary breakthrough curves were obtained for different CO<sub>2</sub> feed compositions, and a mathematical model was applied to predict the dynamic behavior of the adsorption bed. The equilibrium selectivity was found to be 54 at 298 K, 2.4 bar, with a gas composition of 10% CO<sub>2</sub> in N<sub>2</sub>.

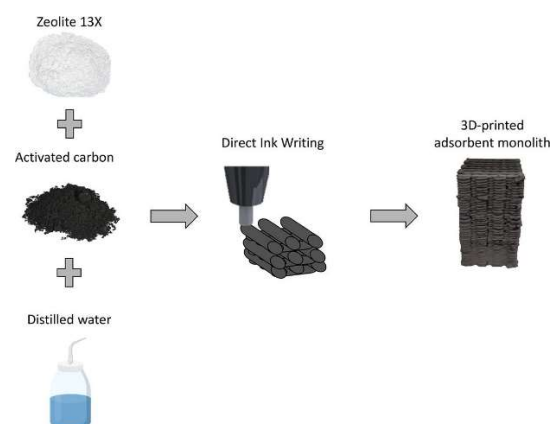


Fig 1. Illustration of the procedure involving the mixing of the raw adsorbents and direct ink writing for the structured adsorbent.

Furthermore, this research focused on the development of an adsorbent material using 3D printing technology, more specifically direct ink writing (DIW). The inks were composed of zeolite 13X, activated carbon (AC), and a binder (Fig. 1). Two compositions were tested: the first with 70%wt. zeolite and 30%wt. activated carbon (AC), and the second is composed of equivalent mass percentages of zeolite and AC. Both 3D-printed materials demonstrated high CO<sub>2</sub> adsorption capacity and electrical conductivity. Yet, the first one exhibited a higher CO<sub>2</sub> adsorption capacity, while the second one demonstrated greater capability to heat upon the application of electric current. The monoliths were printed and characterized, showing promising results in terms of adsorption capacity, mechanical strength, and efficient heating through the Joule effect. The monolith with an equal mass composition of zeolite and AC underwent a more comprehensive analysis of its properties. In addition to CO<sub>2</sub> and N<sub>2</sub> adsorption equilibrium measurements, the dynamics of adsorption was studied. During the adsorption dynamic tests, when subjected to electric current, the material demonstrated accelerated

regeneration through Joule heating, achieving an average desorption rate of  $0.27 \text{ mol} \cdot \text{kg}^{-1} \cdot \text{min}^{-1}$ . The material reached 373 K within approximately 100 s or less in experiments with helium and nitrogen, further confirming the suitability of the monolith for ESA processes.

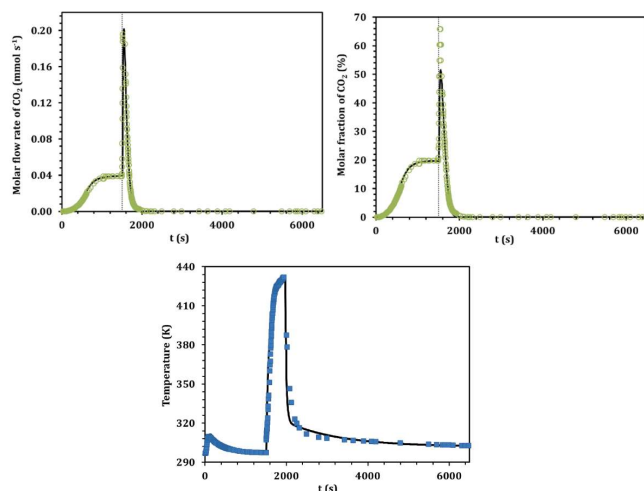


Fig 2.  $\text{CO}_2/\text{He}$  breakthrough experiments. Variation of the molar flow rate of  $\text{CO}_2$  exiting the column, variation of the molar fraction of  $\text{CO}_2$  exiting the column, and temperature history at the first centimeter of the monolith. The symbols are the experimental points, and the line is the simulation results obtained with the mathematical model.

With this monolith, one more valuable conclusion is that the monolith shows adsorption–desorption recyclability when using electric current to regenerate the structured adsorbent. Only a slight loss of capacity is observed (see Figure 3). This is essential for the implementation of the material in a large-scale cyclic adsorption-based process, like ESA.

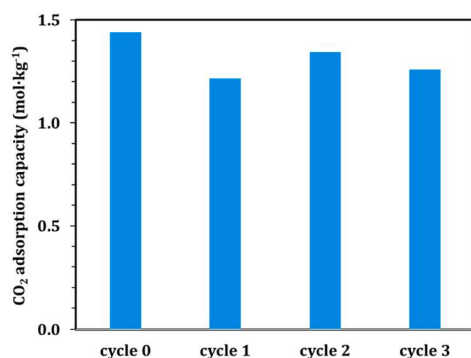


Fig 3.  $\text{CO}_2$  adsorption capacity of the 3D-printed monolith over the cycles.

To explore the impact of composition on shaped materials, we developed new hybrid materials using extrusion for ESA processes. Four mixtures with different contents of AC, zeolite 13X, CMC, and water, were used to produce four different samples: 100% of AC, 70% of AC and 30% of zeolite 13X, 50% of AC and 50% of zeolite 13X, and 30% of AC and 70% of zeolite 13X. The adsorption equilibrium isotherms at 303, 333, and 373 K were measured for all materials, and the experimental data was fitted with the DSL model. As an illustration, the isotherms of the pellets with 50% of AC and 50% of zeolite 13X are presented in Fig. 4. The shaped pellets with higher zeolite composition demonstrated significant  $\text{CO}_2/\text{N}_2$  selectivity. The pellets were subjected to electric current to evaluate the capability of these materials to heat by the Joule effect. Some of the pellets faced challenges in heat regeneration during the ESA process, highlighting the importance of meticulous material selection. Based on the findings, the 50% AC–50% 13X

pellets arose as the most appropriate choice for ESA, considering both adsorption capacity and responsiveness to electrification-induced heating.

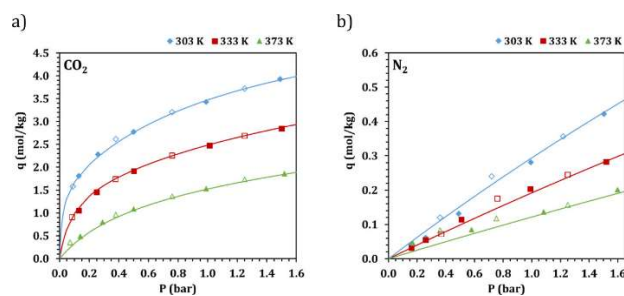


Fig 4. Adsorption equilibrium isotherms of (a)  $\text{CO}_2$  and (b)  $\text{N}_2$  on 50% AC–50% 13X pellets: experimental points (closed adsorption, open desorption) at 303 K (blue diamonds), 333 K (red squares), and 373 K (green triangles) and dual-site Langmuir isotherm fitting (lines)

## Future Perspectives

The 3D-printing process could benefit from enhancements in layer precision and thickness, leading to improved material finishing and overall perfection. Additionally, this improvement would enable the construction of honeycomb monolith structures with greater length. To establish electric current percolation, a single consolidated piece is crucial, rather than multiple monoliths packed into columns. Hence, acquiring expertise in the 3D-printing process is crucial for advancing the development of materials with larger dimensions.

Addressing the efficiency of electrode heating stands as another significant challenge. As outlined in the research conducted previously, electrification at higher electric power proves to be more energetically advantageous due to accelerated heating and reduced energy losses.

## Related Sustainable Development Goals



## Outputs

### PhD Theses

- [1] Maria João Barbosa Regufe,  $\text{CO}_2$  Capture from Flue Gases by Electric Swing Adsorption, PDEQB, FEUP, 2019
- [1] Ana Jorge Meireles Pereira, Additive Manufacturing of Structured Adsorbents for Adsorption-based Processes, PDEQB, FEUP, Ongoing

### Selected Publications

- [1] M. J. Regufe *et al.*, *Adsorption* 24, 249–265 (2018).
- [2] M. J. Regufe *et al.*, *Microporous and Mesoporous Materials* 278, 403–413 (2019)
- [3] M. J. Regufe *et al.*, *Industrial & Engineering Chemistry Research* 59, 12197–12211 (2020)
- [4] A. Pereira *et al.*, *Chemical Engineering Journal* 450, 138197 (2022)
- [5] A. Pereira *et al.*, *Journal of Advanced Manufacturing and Processing* 4, e10108 (2022)

## Team

**Alírio E. Rodrigues**, Emeritus Professor; **José Miguel Loureiro**, Associated Professor; **Alexandre Ferreira**, Assitant Professor / Group Leader; **Ana Mafalda Ribeiro**, Assitant Professor; **Maria João Regufe**, *Ph.D.* student and PostDoc Researcher; **Ana Pereira**, *Ph.D.* Student.

## Funding

- LSRE-LCM Base Funding, UIDB/50020/2020, 2020-2023
- LSRE-LCM Programmatic Funding, UIDP/50020/2020, 2020-2023
- LA LSRE-LCM Funding, UID/EQU/50020/2019, 2019
- LA LSRE-LCM Funding, POCI-01-0145-FEDER-006984, 2013-2018
- NORTE-01-0145-FEDER-000006
- NORTE-01-0145-FEDER-000077
- NORTE-01-0145-FEDER-000054
- FCT Scholarships: PD/BD/105981/2014
- FCT Scholarships: 2022.10612.BD

# Cyclic Adsorption Processes

## Gas Phase Separation Processes

### Simulated Moving Bed: olefins/paraffins

**KEYWORDS:** Adsorption / Simulated moving bed / Separation / Ethylene / Propylene

In the period of this report, different Simulated Moving Bed (SMB) processes were developed for the complete separation of olefins/paraffins. Namely, six experimental SMB separations of light hydrocarbons using four different adsorbents (Cu-BTC, ZIF-8, zeolite 13X monoliths, and zeolite 13X beads).

#### Introduction

From the various products obtained from crude oil, high value is given to light olefins and aromatics because these are the building blocks for a wide range of materials such as plastics, resins, fibers, elastomers, lubricants, and detergents. From the light olefins produced, ethylene and propylene stand out, with global demand of 164 million tons of ethylene and 114 million tons of propylene in 2019. In 2021, ethylene and propylene combined accounted for 54 percent of the global primary petrochemical consumption. Ethylene is expected to grow by 6 % between 2022 and 2030, and propylene by 4.1 %. Ethylene is one of the most profitable products that crude oil can provide. It is produced on such a large scale that often is used as a benchmark for the performance of the petrochemical industry as a whole, and nearly 62 % of its demand belongs to its application in polyethylene production. The primary application of this polymer is in film applications for packaging, carrier bags, and bin/trash liners. While injection molding, pipe extrusion, wire and cable sheathing, insulation, and extrusion coating of paper and cardboard, represent other applications. The second most important product is propylene. More than 60 % of the world's propylene is used to make polypropylene, one of the petrochemical industry's most widely-used and versatile products. Propylene can be found in countless end-use products, including automotive components, carpets, computer disks, eyeglasses, clear film food wrap, flexible and rigid foams, molded plastic goods such as buckets, glazing, food containers, kitchen utensils and wastebaskets, nitrile rubber hoses, seals and gaskets, paints and protective coatings, grocery bags, synthetic fibers, and wood products such as plywood and laminates. To produce polymer-grade light olefins, 99.9 % purity is required for ethylene and 99.5 % purity for propylene, so a purification process should proceed with the production step. Cryogenic distillation is the most commonly used technology. Since the compounds that must be separated have very similar boiling points, C2-splitter and C3-splitter distillation towers, containing between 100 - 130 plates and operating at a very high reflux ratio, are needed to perform the separations. These conditions make these two separations the most cost-intensive separation processes in the petrochemical industry.

Since the 1990s, several other separation processes based on adsorption, absorption, and permeability principles have been studied and developed. Given the extent of the light olefins market, as explained before, improvements in the separation process will significantly reduce operation costs.

The objective of the present work is to study light olefins separation by cyclic adsorptive processes, particularly the gas-phase Simulated Moving Bed (SMB) technology. This study consists of studying an alternative technology to cryogenic distillation and testing new materials such as MOFs (Metal Organic Frameworks) and other materials designed to make

cyclic adsorptive technology an alluring candidate for the process state of the art.



Fig. 1. Experimental set-up of the gas phase simulated moving bed.

#### Current Development

The recovery of ethylene as a product from ethylene/ethane mixtures by adsorptive processes has been attracting great interest due to the high operating and capital costs of the cryogenic distillation traditionally practiced. This search for novel economical ways to separate olefins from paraffins by adsorptive processes has motivated the appearance of improved materials. The trend of developing new materials, such as metal-organic frameworks (MOF), and the challenge of improving the existing technologies, such as pressure swing adsorption (PSA) and simulated moving bed (SMB) leave the horizon open for new alternatives. PSA and SMB in the gas phase were tested to produce ethylene at high purity on Cu-BTC MOF in bead form. For the first time, the olefin/paraffin separation by SMB technology, using an MOF as an adsorbent, was achieved. Both technologies were successfully implemented experimentally and simulated. In the best cycle performed by VPSA for the 20/80 ethane/ethylene feed composition, the ethylene was obtained with a purity of 98.0% at a recovery of 70.2% and a productivity per unit mass of stationary phase of  $1.55 \text{ mol}_{\text{C}_2} \text{ h}^{-1} \text{ kg}^{-1}_{\text{adsorbent}}$ . Additionally, for the 50/50 ethane/ethylene mixture only 43.2% of the ethylene is recovered at a purity of 95.4% and a productivity of  $0.52 \text{ mol}_{\text{C}_2} \text{ h}^{-1} \text{ kg}^{-1}_{\text{adsorbent}}$ . In two cycles performed by SMB, to separate 39/61 ethane/ethylene mixture, ethylene was obtained with a purity of 95%, a recovery above 90%, and productivity between 0.50 and  $0.66 \text{ mol}_{\text{C}_2} \text{ h}^{-1} \text{ kg}^{-1}_{\text{adsorbent}}$ . All the experiments were well predicted by the axial dispersion flow model with the LDF approximation.

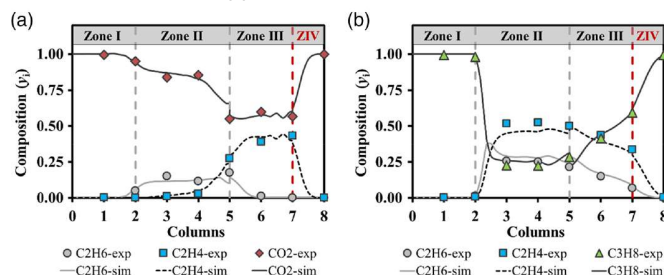


Fig. 2 - Internal profile obtained at the middle of the switching time for (a)  $\text{CO}_2$  and (b)  $\text{C}_3\text{H}_8$ , both at cyclic steady state. Points correspond to experimental data and lines represent the simulation results.

Addressing the same separation (ethane/ethylene) two simulated moving bed (SMB) cycles were employed to separate mixtures containing of about 40% of ethane and 60% of ethylene on zeolitic imidazole framework-8 granulates. The separation cycles were performed with two desorbents with different relative adsorption strengths. In the experiment, with carbon dioxide as desorbent, ethylene was obtained with 99.6% purity and 94.2% recovery, while in the experiment using propane as desorbent only 77.1% of ethylene was recovered with a purity of 82.7%. Indeed, it can be concluded that when CO<sub>2</sub> is used as desorbent, the obtained productivity is higher (see Figure 2). The mathematical SMB model and regions of separation were determined for each desorbent based on experimental data.

Another important case study is the separation of propane and propylene. In this study, carbon dioxide was used as a desorbent and binderfree zeolite 13X as adsorbent in the SMB. The process occurred at a mild temperature (323 K) using the gas-simulated moving bed (SMB) technology. Adsorption equilibrium isotherms of propylene, propane, and carbon dioxide were measured gravimetrically in a temperature range from 323 to 423 K and a pressure up to 5 bar. Breakthrough experiments were performed at 323 K and 3 bar. Binary adsorption equilibrium data were obtained from the dynamic experiments. Non-ideal adsorption behavior was observed for the adsorbate-adsorbent pairs; therefore, the multicomponent adsorption equilibrium was predicted with the RAST-aNRTL model. An SMB experiment was performed in the gas-SMB unit. For the 0.5/0.5 propane/propylene (molar-based) feed composition, a propylene purity of 98.8% was obtained, with a recovery above 98% and a productivity of 40.8 kg<sub>C<sub>3</sub>H<sub>6</sub></sub> h<sup>-1</sup> m<sub>ads</sub><sup>-3</sup>. This work experimentally demonstrated that it is possible to produce high-purity propylene with a high recovery using binderfree zeolite 13X as adsorbent and carbon dioxide as a desorbent at mild temperature (323 K).

With the same adsorbent in the monolith form, the separation of ethane/ethylene was again addressed. In this work, binderfree zeolite 13X monoliths were tested as a new promising material for high-purity ethylene production from olefin/paraffin mixtures by gas-SMB technology.



Fig. 3 - Binderfree zeolite 13X monolith.

To characterize the adsorbent and its potential for the target separation, the equilibrium isotherms of ethane, ethylene, and propane were measured gravimetrically, in a temperature range from 323 K to 423 K, and pressure up to 7 bar. Dynamic studies were performed at 373 K and 1.5 bar in the gas-SMB bench-scale unit. For the experiment with 0.48/0.52 ethane/ethylene (molar based) feed composition, an ethylene purity of 97.7% was obtained, with a recovery above 90% and productivity of 16.9 kg<sub>C<sub>2</sub>H<sub>4</sub></sub> h<sup>-1</sup> m<sub>bed</sub><sup>-3</sup>. Furthermore, the mathematical SMB model and the regions of separation were determined based on experimental data. This work experimentally demonstrated it is possible to produce high purity grade ethylene with a high recovery using binderfree zeolite 13X monoliths as adsorbent and propane as desorbent.

Furthermore, the downstream separations required for the SMB process to obtain polymer-grade products was addressed in a study with MIL-100(Fe) as adsorbent in a PSA process. The main objective of this work is the separation of 0.30/0.70 ethane/propane and 0.30/0.70 ethylene/propane by pressure swing adsorption (PSA) on MIL-100(Fe). The metal-organic framework MIL-100(Fe) was proposed as a potential adsorbent due to its high C<sub>2</sub>/C<sub>3</sub> selectivity. Since adsorption equilibrium data are essential for the process design, the adsorption isotherms of ethane, ethylene, and propane were measured at 323, 373, and 423 K by a gravimetric method. Fixed-bed experiments were conducted at 0.5 SLPM, 323 K, and 150 kPa feed conditions on a bench-scale vacuum PSA (VPSA). Equilibrium and dynamic studies confirmed the preferential adsorption of propane over ethane and ethylene, with a high adsorption separation factor. Two five-step VPSA cycles with two different feed compositions, 0.30 ethane/0.70 propane, and 0.30 ethylene/0.70 propane, at 323 K and 150 kPa on MIL-100(Fe) were designed and performed experimentally. The performance parameters demonstrated the high viability of the proposed processes, since ethane purity of 99.5% was achieved, and with a high ethane recovery (86.7%). In the same cycle, 99.4% of propane was recovered with 97.0% purity. In cycle scheme 2, an ethylene purity of 100.0% was achieved. The propane was 100% recovered with a purity of 94.7%.

#### Future Perspectives

The results obtained revealed that SMB is a viable, competitive alternative to the currently used cryogenic distillation process. In this way, LSRE activities will continue in this area exploring potential new adsorbents and/or new designs to respond to relevant industrial problems separations.

In future work, it was proposed to further exploit this process, focusing on the research of novel adsorbents and more efficient SMB processes capable of operating in a more energy-efficient way.

#### Related Sustainable Development Goals



#### Outputs

##### PhD Theses

- [1] Vanessa Filomena Duarte Martins Light Olefin/Paraffin Separation By Cyclic Adsorption Processes, PDEQB, FEUP, 2019
- [2] Rute Agostinha Gomes Seabra Separation of light hydrocarbons by Simulated Moving Bed, PDEQB, FEUP, 2023

##### Selected Publications

- [1] V. F. Martins *et al.*, Adsorption 24, 203–219 (2018)
- [2] V. F. Martins *et al.*, AIChE J 65, e16619 (2019)
- [3] R. Seabra *et al.*, Chemical Engineering Science 229, 116006. (2021)
- [4] R. Seabra *et al.*, Industrial & Engineering Chemistry Research 62, 12600-12612 (2023)

#### Team

**Alírio E. Rodrigues**, Emeritus Professor; **José Miguel Loureiro**, Associated Professor; **Alexandre Ferreira**, Assitant Professor / Group Leader; **Ana Mafalda Ribeiro**, Assiatnt Professor; **Maria João Regufe**, Junior Researcher; **Vanessa Martins**, Ph.D. Student; **Rute Seabra**, Ph.D. Student; **Rafael Dias**, Ph.D. Student;

#### Funding

LSRE-LCM Base Funding, UIDB/50020/2020, 2020-2023  
 LSRE-LCM Programmatic Funding, UIDP/50020/2020, 2020-2023  
 LA LSRE-LCM Funding, UID/EQU/50020/2019, 2019  
 LA LSRE-LCM Funding, POCI-01-0145-FEDER-006984, 2013-2018  
 AIProcMat@N2020, NORTE-01-0145-FEDER-000006, 2016-2019  
 LSRE-LCM, POCI-01-0145-FEDER-006984  
 ALiCE, LA/P/0045/2020

# Cyclic Adsorption Processes

## Gas Phase Separation Processes

### Gas-Phase Simulated Moving Bed: Methane/Nitrogen Separation

**KEYWORDS:** Separation, Adsorption, Vacuum pressure swing adsorption, Simulated moving bed, CH<sub>4</sub>/N<sub>2</sub> separation

**For the separation of methane and nitrogen mixtures, the performance of several materials were tested, including activated carbons and metal-organic frameworks. Also, different adsorption-based processes were developed, such as improved vacuum pressure swing adsorption (VPSA) and gas-phase simulated moving bed (SMB) processes, as potential alternatives to cryogenic distillation for small/medium-scale production of purified methane streams.**

#### Introduction

As a result of the rising demand for natural gas, the exploration of unconventional methane-rich sources has been gradually increasing over the years due to the depletion of the conventional wells. These sources are often contaminated with several impurities, among which nitrogen is the most challenging to be removed, owing to its similar properties to those of methane.

When the nitrogen concentration is above 3%, its removal becomes necessary to ensure that the calorific value of the stream is not affected by the presence of this inert gas. The main technology used for this purpose involves multi-stage distillation columns, operating at cryogenic temperatures to liquefy the methane gas, allowing the nitrogen to be rejected from the stream, which has very high energy costs associated. When compared to this cryogenic distillation technology, adsorption-based processes are very appealing thanks to their easy scalability and low equipment and operating costs. However, the performance of the solid materials for CH<sub>4</sub>/N<sub>2</sub> separation becomes an issue due to their low adsorption selectivity. This way, research of novel materials and alternative strategies for the upgrade of methane is of utmost importance. Improving the traditional VPSA process can be one of these strategies, by implementing displacement desorption to recover low-grade methane in a more economic and efficient way. The use of a gas-SMB process can also be an alternative process, as it can separate mixtures with selectivities close to unity by introducing a desorbent to displace the adsorbed phase, transforming a difficult separation into two easier ones. This way, choosing the appropriate adsorbent/desorbent pair is essential for efficient separation. The desorbent must be able to displace the adsorbed phase and be displaced by the gaseous mixture. Also, it should differ in properties from the compounds present in the gas mixture so that the separation of the SMB extract (more retained species + desorbent) and raffinate (less retained species + desorbent) streams is easily achieved.

#### Current Development

To upgrade efficiently a low-concentration methane gas from nitrogen mixture, a VPSA process was employed with CO<sub>2</sub> displacement (VPSA-CO<sub>2</sub>DIS). Non-isothermal and non-isobaric mathematical model for the VPSA-CO<sub>2</sub>DIS process was developed, where ternary competitive adsorption equilibrium of CH<sub>4</sub>, N<sub>2</sub> and CO<sub>2</sub> was calculated using IAST-Sips formulation, and bi-pore diffusion model was used to describe adsorption kinetics. Experiments were carried out to enrich the low-grade methane gas using one-bed four-step VPSA-CO<sub>2</sub>DIS process with the home-made granular activated carbons (GACs), and results compared to process simulation predictions. Both experimental and simulated results

confirmed that a high purity CH<sub>4</sub> product gas (75.40% CH<sub>4</sub>) could be obtained continuously from 10% CH<sub>4</sub> feed gas with 89.02% recovery.

For the same purpose, an improved VPSA process with SMB operation was also studied. To run this process automatically, the SMB operation mode was introduced, synchronously shifting the inlet and outlet stream ports along the gas flow direction, ensuring countercurrent contact between gas and solid phase to enhance the CH<sub>4</sub>/N<sub>2</sub> separation. To verify its feasibility, the experimental device with an eight-column unit had been set up in laboratory, and 30% ~ 50% CH<sub>4</sub> gases were denitrified by the improved VPSA process using activated carbon beads. Results have shown that this process was capable of producing a high-purity CH<sub>4</sub> product gas (99.99% CH<sub>4</sub>) meeting pipeline grid specification and a high-concentration N<sub>2</sub> by-product gas meeting emission standards from 30% ~ 50% CH<sub>4</sub> feed gases. In the end, we compared the CH<sub>4</sub>/N<sub>2</sub> separation performance among the conventional VPSA, dual reflux-PSA, improved VPSA with SMB operation, CO<sub>2</sub> displacement VPSA, and concentration temperature swing adsorption (CTSA).

Another displacement VPSA process was devised for simultaneous methane recovery from CH<sub>4</sub>/N<sub>2</sub> and CH<sub>4</sub>/CO<sub>2</sub> mixtures. The process comprises seven steps, involving pressurization, adsorption, displacement, depressurization, blowdown under vacuum pressure, and two purges under vacuum pressure. This separation yielded three gases: a CH<sub>4</sub>-rich product at the displacement step, N<sub>2</sub>-rich by-product at adsorption, and CO<sub>2</sub>-rich by-product at blowdown. Experimental tests with a coconut shell activated carbon adsorbent confirmed high-purity methane product gas (~ 95.0% CH<sub>4</sub> purity) from both mixtures. A mathematical model was developed to predict gas compositions and assess the impact of CO<sub>2</sub> in CH<sub>4</sub>/N<sub>2</sub> on the separation performance. Both experimental and numerical results support the effectiveness of the proposed process.

Two MOFs, the ZIF-8 (Basolite Z1200) and MIL-53(Al) (Basolite A100) were shaped employing the extrusion method with the purpose of studying their performance for nitrogen rejection from methane streams. For that, two binders were used: alumina and carboxymethylcellulose (CMC). Loadings of 5, 10, and 15 %wt. of alumina were utilized to shape ZIF-8 and MIL-53(Al) into pellets. Additionally, pellets of ZIF-8 with 5 and 10 %wt. of CMC were also produced. The materials were characterized by SEM/EDS, N<sub>2</sub> adsorption at 77 K, CO<sub>2</sub> adsorption at 273 K, mercury intrusion porosimetry, and XRD to evaluate the effect of the shaping process on the materials. The shaping process does not result in significant alterations in the crystalline structure of the materials. Generally, an increase in binder quantity led to a decrease in average pore diameter and surface area. Crush strength tests indicated improved mechanical strength with higher binder amounts. The adsorption equilibrium isotherms for CH<sub>4</sub> and N<sub>2</sub> were determined at 303 K up to 4 bar. Langmuir adsorption model was used to fit the experimental results. This study allows understanding the effect of shaping in the adsorption capacities of the materials. For both gases, the impact of shaping in the adsorption capacities is higher on the MIL-53(Al) materials than on ZIF-8 pellets.

Besides VPSA processes, the gas-phase simulated moving bed technology was also researched. Firstly, a functionalized zirconium-based metal-organic framework, the UiO-66(Zr)<sub>2</sub>(COOH)<sub>2</sub>, supplied by KRICT, was tested to be used in a gas-phase simulated moving bed (SMB) process. Adsorption equilibrium data for ethane was measured and compared with previously measured data for CH<sub>4</sub>, N<sub>2</sub>, and CO<sub>2</sub>. Single, binary, and pseudo-ternary breakthrough curves were performed at 333 K and 1.5 bar. These experimental results allowed experimental validation of adsorption equilibrium predicted by the multicomponent extension of the DSL isotherm and the validation of the fixed-bed mathematical model, as well as the evaluation of the ability of the eluent of displacing the mixture and its own displacement by the mixture. Lastly, a gas-phase SMB process was designed, based on the simulation of the separation regions for each one of the target desorbents, operating at 303 K and 1.5 bar, using four-zone unit configuration (2–3–2–1), in a closed-loop. This process allows the production of a methane stream with 99.56% purity and 99.65% recovery and a nitrogen stream with 99.73% purity and a recovery of 99.58%.

An SMB process for the separation of methane and nitrogen mixtures was also developed, using a commercial activated carbon (BPL) as the adsorbent material and two potential desorbent gases: argon and carbon dioxide. The pure component isotherms of N<sub>2</sub>, CH<sub>4</sub>, Ar, and CO<sub>2</sub> were measured at 303, 323, and 343 K in a pressure range of 0–2.5 bar using a volumetric apparatus, with CO<sub>2</sub> exhibiting the highest affinity to the stationary phase and Ar the lowest. The data was regressed against the dual-site Langmuir (DSL) model. Single, binary, and ternary breakthrough curves were also assessed, allowing the validation of the proposed mathematical model. Two SMB cycles were employed to separate an equimolar CH<sub>4</sub>/N<sub>2</sub> mixture using each desorbent gas to evaluate the impact of the desorbent strength in the process. The respective separation regions were drawn. Both cycles were capable of producing a high-purity methane stream (96.2 and 97.4% for the Ar and CO<sub>2</sub> experiment, respectively) with high recovery (>92%). When argon is used as the desorbent gas, the extract product stream is obtained with a productivity of 14.1 kg·m<sup>-3</sup><sub>ads</sub>·h<sup>-1</sup>.

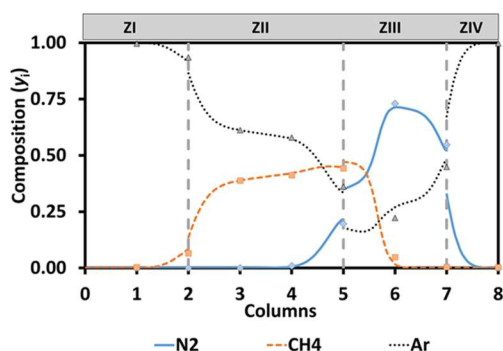


Fig. 1. Internal profile at 50% of switching time for the SMB cycle using the BPL/Argon adsorbent/desorbent pair.

Lastly, to aid in the selection of potential materials for this separation, an SMB performance indicator (SPI) was developed. In a simulated moving bed, the regeneration is accomplished by the introduction of a third species, the desorbent, which is later recovered by two downstream separations. As such, the choice of a proper adsorbent/desorbent pair is critical to ensure the effectiveness of the SMB process. By developing a parameter that uses readily available literature data, the selection process is sped up, while diminishing the computational effort required. This indicator involves the trade-off between the adsorption selectivity in the presence of the desorbent, the adsorption

capacity of the most retained species, and the ratio of the most and less retained species' enthalpies.

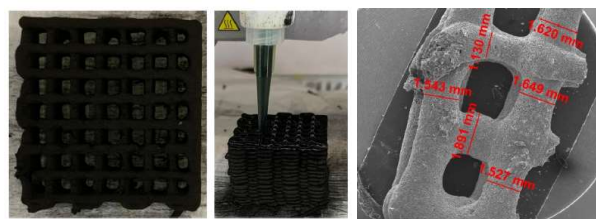


Fig. 2. 3D-printed activated carbon monolith

Maxsorb, one of the adsorbents highlighted by the SPI, was used to fabricate a monolithic structure containing a small amount of CMC (10%wt.) as a binder using the DIW technique. Monoliths were characterized in terms of surface area, pore volume, and pore size distribution. Afterward, the ability of the 3Dprinted monolith to separate N<sub>2</sub> from the CH<sub>4</sub>, for methane upgrading was tested. The textural and adsorptive properties were compared with the ones of its pristine powder. In conclusion, the first 3D-printed monolith for CH<sub>4</sub>/N<sub>2</sub> separation was developed in this work, and the structured adsorbent was shown to be a candidate for this separation.

### Future Perspectives

The future prospects for this research topic include the research of more efficient materials for methane/nitrogen separation, as well as optimizing and improving the gas-SMB process to be implemented at an industrial scale. The downstream separation by PSA of the desorbent from the extract and raffinate product streams will also be a case study, as it is an essential step to obtain pure components.

### Related Sustainable Development Goals



### Outputs

#### PhD Theses

[1] Rafael Osório Marques Dias, Gas-phase simulated moving bed for methane upgrade, PDEQB, FEUP, Ongoing

#### Master Dissertations

[1] Ana Jorge Meireles Pereira, Shaping, characterization, and measurement of adsorption properties of ZIF-8 and MIL 53(Al) adsorbents, MIEQ, FEUP, 2019  
 [2] Rafael Osório Marques Dias, Gas-phase simulated moving bed for methane and nitrogen separation, MIEQ, FEUP, 2019

#### Selected Publications

[1] D. Qu *et al.*, Chemical Engineering Journal 380, 122509 (2020)  
 [2] Z. Qian *et al.*, Chemical Engineering Journal 419, 129657 (2021)  
 [3] R. O. Dias *et al.*, Brazilian Journal of Chemical Engineering 39, 973-990 (2022)  
 [4] Y. Zhou *et al.*, Fluid Phase Equilibria 561, 113541 (2022)  
 [5] R. O. Dias *et al.*, Industrial & Engineering Chemistry Research 61, 12739-12753 (2022)  
 [6] A. Pereira *et al.*, Microporous and Mesoporous Materials 331, 111648 (2022)  
 [7] R. O. Dias *et al.*, AIChE Journal 69, e18074 (2023)

#### Team

**Alúrio E. Rodrigues**, Emeritus Professor; **Ana Mafalda Ribeiro**, Assitant Professor; **Alexandre Ferreira**, Assistant Professor / Group Leader; **Idelfonso Nogueira**, Junior Researcher (now at NTNU); **Maria João Refuge**, Junior Researcher; **Rafael Dias**, Ph.D. Student; **Ana Pereira**, Ph.D. Student;

#### Funding

SiMoBedMethaSep, NORTE-01-0145-FEDER-029384, 2018-2021  
 LSRE-LCM Base Funding, UIDB/50020/2020, 2020-2023  
 LSRE-LCM Programmatic Funding, UIDP/50020/2020, 2020-2023  
 LA LSRE-LCM Funding, UID/EQU/50020/2019, 2019  
 LA LSRE-LCM Funding, POCI-01-0145-FEDER-006984, 2013-2018  
 ALICE, LA/P/0045/2020  
 LSRE-LCM, POCI-01-0145-FEDER-006984  
 FCT Grants: 2020.05095.BD, 2020-2023

# Cyclic Adsorption Processes

## Gas Phase Separation Processes

### Membrane separations: H<sub>2</sub> purification + O<sub>2</sub>/O<sub>3</sub> separation

**KEYWORDS:** Gas Separation / Hydrogen / Oxygen / Ozone / Membrane / Modeling/ Permeation / PDMS/ Titanosilicate

Membrane technology as a gas separation process has grown considerably in recent years since they are small, simple, and easy to operate systems and the membranes can be adapted to suit separation needs. This research group has focused on investigating the separation of O<sub>2</sub>/O<sub>3</sub> and hydrogen purification through membrane-based processes. The experimental results disclosed high selectivity of the AM-3 membrane towards hydrogen. The calculated results demonstrated that: viscous flow prevailed at low temperature (304 K), surface diffusion dominated when temperature increased, Knudsen transport was residual, the flux through defects predominated at 304 K (53.8–73.5% of total flux), and the influence of the support was negligible. Regarding O<sub>2</sub>/O<sub>3</sub> separation only a few preliminary tests have been carried out but it is expected that the membranes prepared will be ozone-resistant in the long term and will be able to increase the ozone concentration from 6 to 10 weight percent, which is equivalent to a selectivity of 1.7 for O<sub>2</sub>/O<sub>3</sub>.

#### Introduction

Membrane technology is a very promising field of separation processes due to the reduction of electricity and fuel consumption, simplicity of operation and installation, and the fact that membranes can be adapted to fit separation requirements (for example incorporating fillers like zeolites, metal–organic frameworks (MOFs), etc.). Relevant industrial applications encompass the following examples: i) separation of N<sub>2</sub> from air; ii) removal of H<sub>2</sub> and CO<sub>2</sub> from natural gas; iii) H<sub>2</sub>/N<sub>2</sub> and H<sub>2</sub>/hydrocarbon separations in ammonia and petrochemical plants; iv) removal of CO<sub>2</sub> from process streams to prevent the “greenhouse effect”; v) removal of volatile organic compounds from air or nitrogen streams; and vi) separation of hydrocarbon isomers in the petrochemical industry.

In this research group, O<sub>2</sub>/O<sub>3</sub> separation and hydrogen purification using membranes have been studied. Synthesized and commercial PDMS membranes have been used for O<sub>2</sub>/O<sub>3</sub> separation to obtain an O<sub>3</sub>-enriched gas stream. Polymeric PDMS membranes are an exciting solution for O<sub>2</sub>/O<sub>3</sub> separation since they exhibit an ozone permeability higher than oxygen, enhancing the purification of the ozone feed stream. Additionally, a new AM-3 membrane was prepared on a stainless-steel support for potential application in the separation of light gases, particularly hydrogen-containing mixtures. AM-3 is a synthetic microporous titanosilicate structurally analog of natural penkvilksite-2O with the ideal formula Na<sub>2</sub>TiSi<sub>4</sub>O<sub>11</sub>·2H<sub>2</sub>O. Taking into account its small pore diameter (0.3 nm), AM-3 can be studied with advantage as effective molecular sieve for gas separations being considered a potential candidate for the separation of hydrogen.

#### Current Development

##### O<sub>2</sub>/O<sub>3</sub> separation

The separation of oxygen and ozone was first studied through the simulation of a permeation system with two different membrane configurations (spiral wound and hollow fiber) and their possible operating flow patterns (cross-flow in the spiral wound membrane, and co-current, counter-current, and cross-

flow in the hollow fiber membrane), with the aim of better understanding the membrane behavior in these modules.

The overall analysis showed that by increasing the membrane permeability of oxygen or ozone, selectivity, membrane dimensions, or feed pressure or decreasing the permeate pressure, it is possible to increase the permeate flux. As for the ozone concentration on the permeate side, it decreases with the increase of the membrane permeability of O<sub>2</sub> or O<sub>3</sub> and the membrane dimensions and increases with the increase of the other parameters. Taking all of this into account, it is necessary to find a balance between all the studied parameters according to the objective of the separation.

In addition, asymmetric PVDF/PDMS flat membranes were synthesized and tested in a flat sheet module. A preliminary assessment of membrane performance was first carried out through single-component tests with oxygen to determine the O<sub>2</sub> permeance. Fig. 1 represents the permeate flow rate of oxygen versus transmembrane pressure for PVDF/PDMS membrane (5 wt.%) in a single-component test with oxygen.

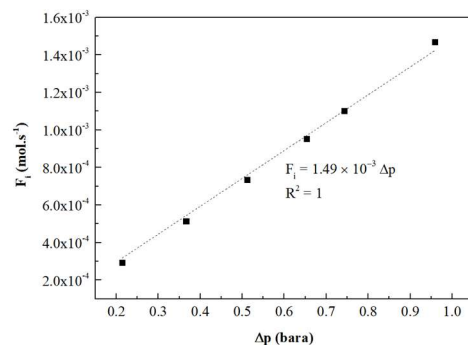


Fig 1. Permeate flow rate versus transmembrane pressure for PVDF/PDMS (5 wt.%) membrane for single-component experiment.

The gas separation laboratory set-up where the gas separation tests were carried out is illustrated in Fig. 2.



Fig 2. Gas separation set-up.

##### H<sub>2</sub> purification

The SEM image of synthesized AM-3 crystals is shown in Fig.3, being possible to conclude that our seeds are plates of ca. 1.0 μm x 0.5 μm.

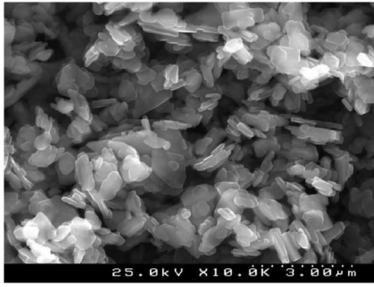


Fig 3. SEM image of AM-3 seeds.

To assess the existence of macro-defects in the AM-3 toplayer of the membrane, a set of thirty measurements was made with nitrogen combining ten temperatures (304–394 K) and three transmembrane pressure drops ( $\Delta P_{\text{tot}} = 0.5, 1.0$  and  $1.5$  bar). The results show a slight and proportional increase of  $N_2$  permeance with increasing  $\Delta P_{\text{tot}}$ , which discloses the small influence of viscous flow contribution typical of macro-defects.

Pure gas permeation experiments were performed under similar conditions ( $\Delta P_{\text{tot}} = 0.5$  bar and ten temperatures from 304 to 394 K) for He,  $N_2$ ,  $O_2$ ,  $CO_2$ , and  $H_2$ . The results are graphically shown in Fig. 4a and point out a common trend – permeances increase with temperature and tend to a maximum. Hydrogen exhibits the highest permeances over the whole temperature range, varying from  $1.30 \times 10^{-7} \text{ mol m}^{-2} \text{ s}^{-1} \text{ Pa}^{-1}$  at 304 K to  $6.53 \times 10^{-7} \text{ mol m}^{-2} \text{ s}^{-1} \text{ Pa}^{-1}$  at 393 K. Over the same temperature interval, helium permeance varies from  $9.26 \times 10^{-8}$  to  $4.59 \times 10^{-7} \text{ mol m}^{-2} \text{ s}^{-1} \text{ Pa}^{-1}$ . Both gases evidence superior permeabilities in comparison to the remaining ones, whose permeance data fall between  $(4.63 - 7.13) \times 10^{-8}$  and  $(1.86 - 2.28) \times 10^{-7} \text{ mol m}^{-2} \text{ s}^{-1} \text{ Pa}^{-1}$ . As a first approximation, this behavior results from the interplay between the small pores of AM-3 membrane and the kinetic diameters of the diffusing species, which globally favors  $H_2$  and He permeation: 0.289 nm ( $H_2$ ) and 0.260 nm (He) versus 0.364 nm ( $N_2$ ), 0.346 nm ( $O_2$ ), and 0.33 nm ( $CO_2$ ). In any case, besides sieving/size effects, gas-solid potential interactions have also to be considered.

The potential of the AM-3 membrane for the separation of hydrogen containing mixtures rely on its selectivity towards hydrogen. In Fig. 4b the ideal selectivities  $\alpha_{H_2,i}$  ( $i=O_2, CO_2, N_2$  and He), defined by the ratio of unary permeances of both gases, are plotted against temperature. The results illustrate that the ideal selectivities are monotone increasing for  $H_2/O_2$ ,  $H_2/CO_2$  and  $H_2/N_2$ , and are essentially constant for  $H_2/He$ : specifically, over the range 304–393 K,  $\alpha_{H_2,O_2}$  increases from 2.82 to 3.50,  $\alpha_{H_2,CO_2}$  from 1.85 to 3.25,  $\alpha_{H_2,N_2}$  from 1.83 to 2.86, while  $\alpha_{H_2,He}$  oscillates around ca. 1.40.

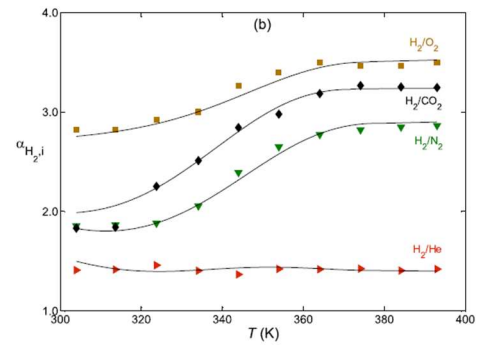
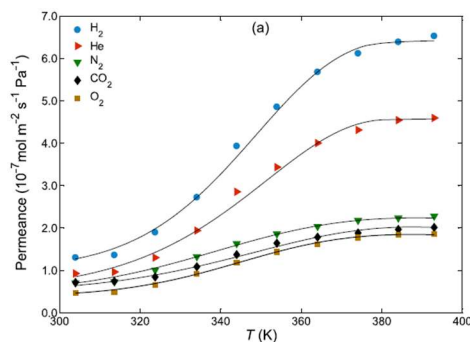


Fig 4. (a) Permeances of pure gases through AM-3 membrane, and (b) ideal selectivities of  $H_2$  over other gases, as function of temperature at  $\Delta P = 0.5$  bar. Symbols: measured data; lines: modeling results.

For the pairs of gases under study one obtains  $\alpha_{H_2,i}^{Kn} = 4.00, 4.69, 3.74$  and  $1.41$  for  $H_2/O_2, H_2/CO_2, H_2/N_2$  and  $H_2/He$ , respectively. Considering the large differences found between experimental and Knudsen selectivity values (except for the pair  $H_2/He$ ), together with their distinct trends with temperature, it is possible to anticipate the low contribution of Knudsen mechanism to the overall permeation.

The modeling results are plotted in Fig. 4b along with the experimental data, revealing the excellent representations achieved in all cases: AARDs between 2.61 and 5.08%, and a global value of only 3.42%.

### Future Perspectives

In the future it is intended to carry out ozone permeation tests in order to calculate  $O_3$  permeation and  $O_2/O_3$  selectivity using flat and spiral wound modules with PDMS membranes. As the ozone concentration in the output of the ozone generator influences energy consumption, it is intended to work with low ozone concentration ranges, around 6 wt.%. It is expected that the membrane system will be able to increase the ozone concentration from 6 to 10 wt.%, which is equivalent to an  $O_2/O_3$  selectivity of 1.7.

### Related Sustainable Development Goals



### Outputs

#### PhD Theses (on going)

[1] Inês Magalhães Rodrigues, Ozone stream purification using customized membranes for  $O_2/O_3$  separation, PDEA, FEUP, ongoing.

#### Master Dissertations

[1] Cristiana Andreia Vieira Gomes, Intensification of ozonation processes for water treatment: ozone/oxygen separation by membrane, MIEQ, FEUP, 2019

#### Selected Publications

[1] S. P. Cardoso et al., Separation & Purification Reviews 27, 229 (2018)  
[2] S. P. Cardoso et al., Microporous and Mesoporous Materials 261, 170 (2018)

#### Team

**Alírio E. Rodrigues**, Emeritus Professor; **Alexandre Ferreira**, Assistant Professor / Group Leader; Vítor Vilar, Principal Researcher; **Cristiana Gomes**, M.Sc. and Ph.D. Student; **Inês Rodrigues**, Ph.D. Student.

#### Funding

OZONE4WATER project, PTDC/EAM-AMB/4702/2020, 2021-2024  
LSRE-LCM Base Funding, UIDB/50020/2020, 2020-2023  
LSRE-LCM Programmatic Funding, UIDP/50020/2020, 2020-2023  
LA LSRE-LCM Funding, UID/EQU/50020/2019, 2019  
LA LSRE-LCM Funding, POCI-01-0145-FEDER-006984, 2013-2018  
FCT Scholarships: 2021.05666.BD and 2022.10784.B